UNIVERSIDAD DE CHILE

FACULTAD DE CIENCIAS QUÍMICAS Y FARMACÉUTICAS

Trypanosoma cruzi CALRETICULIN EXPRESSION IN PARASITES INFECTING MURINE MACROPHAGES

Tesis para optar al grado académico de Doctor en Bioquímica.

ANDREA ELIZABETH GONZÁLEZ ZÚÑIGA

Directores de Tesis

Prof. Dr. Arturo Ferreira V.
Prof. Dr. Norbel Galanti G.

Santiago de Chile
Marzo, 2014

UNIVERSIDAD DE CHILE
FACULTAD DE CIENCIAS QUÍMICAS Y FARMACÉUTICAS

INFORME DE APROBACIÓN
TESIS DE DOCTORADO

Se informa a la Dirección de Postgrado de la Facultad de Ciencias Químicas y Farmacéuticas que la Tesis de Doctorado presentada por la candidata:

ANDREA ELIZABETH GONZÁLEZ ZÚÑIGA

Ha sido aprobada por la Comisión Informante de Tesis como requisito para optar al grado de Doctor en Bioquímica, en el examen de defensa de Tesis rendida el día _____

Directores de Tesis:

Dr. Arturo Ferreira _____

Dr. Norbel Galanti _____

Comisión Informante de Tesis:

Dra. María Antonieta Valenzuela (Presidente) _____

Dr. Ángel Oñate _____

Dra. Monica Imarai _____

Dra. Carmen Romero _____

Dedicado a mis Padres, Aurora y Carlos y a mis abuelitos Carmen y Ramón, porque siempre seran lo más valioso en mi vida, y quienes me han hecho lo que soy.

ACKNOWLEGMENTS- AGRADECIMIENTOS

Esta, probablemente, será la única sección en toda mi Tesis (salvo el resumen) en español. Y también la última página que escribo de mi Tesis Doctoral.

Ha sido un largo camino, a veces más largo del que uno puede presuponer, para ver materializado este trabajo.

Tantos recuerdos vienen a mi mente en este momento, todo lo que ha pasado para poder llegar a este momento, el cierre de un ciclo, el cierre de una etapa, para iniciar otra, que espero sea tan productiva y llena de aprendizajes como esta.

Sin duda, muchas personas a lo largo de estos años han sido un apoyo y han contribuido de una u otra manera a concretar esta Tesis.

En primer lugar, agradezco muy especialmente a mis papás, Aurora y Carlos, quienes con su amor y apoyo incondicional permitieron que pudiese concluir esta etapa de la mejor manera posible. Siempre creyeron en mi, aún en los momentos más difíciles, y sin su ayuda y apoyo hubiera sido imposible acabar esta Tesis. A mis abuelitos, Carmen y Ramón, porque siempre creyeron en mi.

A mis Directores de Tesis, los Dres. Arturo Ferreira y Norbel Galanti, quienes con su guía me han formado, no sólo en el ámbito académico, sino también en el personal, durante esta etapa crucial en mi carrera científica, en especial el Dr. Ferreira, quien me recibió en su laboratorio, creyendo en mi en todo momento, y de quien he aprendido muchísimo en estos años, además de haber sido un soporte en los momentos difíciles.

A los miembros de mi Comisión, los Dres. María Antonieta Valenzuela, Carmen Romero, Mónica Imarai y Ángel Oñate, quienes me acompañaron en el curso de todo este trabajo, con sus sugerencias y comentarios en cada presentación contribuyeron en gran medida mejorar este trabajo. Muy especialmente agradezco a la Dra. Valenzuela quien durante un periodo de tiempo gentilmente me recibió en su laboratorio, siempre con un consejo y palabras de apoyo, y a la Dra. Romero, pues su sugerencia y consejo fueron vitales para sortear con éxito una difícil etapa.

A todos mis compañeros e integrantes del Laboratorio de Inmunología de la Agresión Microbiana, Paula Abello, Jaime Peña, Haydeé Gallardo, Ismael Maldonado, Lorena Aguilar, Gerardo Vallejos, Eduardo Sosoniuk, Javier Pizarro, Katherine Wainberguer, Carolina Valk, Carlos Rosas, Juana Orellana y Ruth Mora.

A todo el Programa Disciplinario de Inmunología, junto a su Director, el Dr. Juan Carlos Aguillón, a la Dra. Karina Pino-Lagos, quien me dio apoyo fundamental en la última parte de este trabajo, a la Dra. Mercedes López, quien siempre tuvo un consejo y una palabra de aliento.

A la Sra. Mari Aranguren, Ana Cepeda, Oriana Córdoba también mi agradecimiento por todo el apoyo prestado tanto en lo administrativo como en lo personal.

A Marta Gacitúa, del Laboratorio de Microscopía Electrónica, quien fue uno de los pilares fundamentales para el desarrollo de este trabajo, donde compartimos todos los éxitos y también las frustraciones. Sin su apoyo este trabajo habría sido imposible.

A los Dres. Soledad Fernández y José Luis Arias, por su apoyo en el análisis de las imágenes de microscopía electrónica.

A la Dra. Gittith Sánchez, otro de los pilares fundamentales de este trabajo, puesto que con sus consejos y apoyo se lograron establecer las condiciones para obtener un material de trabajo óptimo. Sus consejos y amplio conocimiento fueron claves para poder perfeccionar y mejorar todo lo relacionado a los parásitos empleados en este trabajo.

También mi especial agradecimiento a la Dra. María Inés Becker, quien cuando lo necesité no dudó en abrirme las puertas de su laboratorio para mis prácticas.

A los Dres. Andrés Barriga y Matías Rivera, quienes brindaron un apoyo importantísimo en el desarrollo de la parte anexa de mi tesis, en experimentos de análisis por Espectrometría de masas y geles bidimensionales.

Al Laboratorio de Análisis de Imágenes Científicas (SIAN), en especial al Dr. Steffen Härtel y Jorge Mancilla, por su apoyo en la cuantificación del número de partículas de oro en las microfotografías.

A CONICYT por el financiamiento al ser otorgadas las becas CONICYT de Estudios de Doctorado en Chile (2008) y de Apoyo a Tesis Doctoral (2010).

Finalmente, quiero dar gracias a Dios y a mi Virgencita por permitirme, a pesar de todas las pruebas, concluir de manera exitosa esta etapa que cierra un ciclo, complejo, pero del cual he adquirido experiencias que atesoraré por el resto de mi vida.

“LA VIDA NO ES FÁCIL, PARA NINGUNO DE NOSOTROS, PERO, ¡QUE IMPORTA! HAY QUE PERSEVERAR, Y SOBRE TODO TENER CONFIANZA EN UNO MISMO. HAY QUE SENTIRSE DOTADO PARA REALIZAR ALGUNA COSA, Y ESA COSA HAY QUE ALCANZARLA, CUESTE LO QUE CUESTE”

Marie Sklodowska-Curie (Premio Nobel de Física, 1903, y Química, 1911)

This work was performed in the Laboratory of Immunology of Microbial Aggression, Immunology Disciplinary Program, Institute of Biomedical Sciences, Faculty of Medicine, University of Chile, with the financial support of FONDECYT grant 1130099 and Associative Research ACT-112, of Dr. Arturo Ferreira V., FONDECYT grant 1130113 of Dr. Norbel Galanti G., and also CONICYT fellowships: For Doctoral Studies in Chile (21080219) and Doctoral Thesis Support (AT 24100233) obtained by Andrea González Zúñiga.

Generated Publications within the context of this Thesis

González, A., Valck, C., Sanchez, G., Härtel, S., Mansilla, J., Ramirez, G., Fernandez, S., Arias, J.L.,*Galanti, N., *Ferreira, A. (2014) "*Trypanosoma cruzi* Calreticulin in Parasites Infecting Murine Macrophages" Submitted.

National and International Congress Presentations

Author(s): González, A., Valck, C., Sanchez, G., Olea, N., Galanti, N., Ferreira, A.
Title: Morfología Ultramicroscópica de Macrófagos Murinos infectados con *Trypanosoma cruzi*
Year: 2010
Country: Chile
Congress: XIII Jornadas Anuales de Parasitología

Author(s): González, A., Valck, C., Sanchez, G., Olea, N., Galanti, N., Ferreira, A.
Title: Morfología Ultramicroscópica de Macrófagos Murinos infectados con *Trypanosoma cruzi*
Year: 2011
Country: Chile
Congress: Congreso Ciencia Joven 2011

Author (s): González, A., Valck, C., Sanchez, G., Galanti, N., Ferreira, A.
Title: Antibodies Generated against *Trypanosoma cruzi* Calreticulin S-Domain Detects Putative Murine Calreticulin Isoform
Year: 2011
Country: Chile
Congress: XXV Reunión Anual de la Sociedad de Biología Celular de Chile.

Author(s): González, A., Valck, C., Sanchez, G., Ramirez, G., Galanti, N., Ferreira, A.
Title: Calreticulina en Macrófagos infectados con Trypanosoma cruzi
Year: 2012
Country: Chile
Congress: Congreso Ciencia Joven 2012

Author(s): González, A., Valck, C., Sanchez, G., Ramirez, G., Galanti, N., Ferreira, A.
Title: Calreticulina en Macrófagos Infectados con *Trypanosoma cruzi*
Year: 2012
Country: Chile
Congress: Simposio Internacional de Enfermedad de Chagas.

Author(s): González, A., Valck, C., Sanchez, G., Ramirez, G., Härtel, S., Galanti, N., Ferreira, A.
Título: Calreticulina de *Trypanosoma cruzi*: ¿es posible su pasaje desde el parásito hacia la célula hospedera infectada?
Year: 2013

Country: Chile
Congress: Congreso Ciencia Joven 2013

Author(s): González, A., Valck, C., Sanchez, G., Ramirez, G., Härtel, S., Galanti, N., Ferreira, A.
Title: Calreticulina de *Trypanosoma cruzi*: ¿es posible su pasaje desde el parásito hacia la célula hospedera infectada?
Year: 2013
Country: Chile
Congress: IV Simposio Internacional de la Enfermedad de Chagas
III Reunión Nacional Integrada Prevencion y Control de la Enfermedad de Chagas
XV Jornadas Anuales de Parasitología

INDEX

FIGURE INDEX

ABBREVIATIONS

Aº	Amstrongs
aa	Aminoacids
ABTS	2-2'-azino-di-(3-ethylbenzthiazoline-6-sulfonic acid)
AP	Alkaline phosphatase
BCIP	5-bromo-4-chloro-3-indolyl phosphate
BSA	Bovine serum albumin
Bufi	Immune buffer
ºC	Degrees Celsius
cms	Centimeters
CRT	Calreticulin
DNA	Deoxyribonucleic acid
eTcCRT	Endogenous TcCRT
ELISA	Enzyme-linked immunosorbent assay
ER	Endoplasmic reticulum
FACS	Fluorescent-activated cell sorting
FBS	Fetal bovine serum
FITC	Fluorescein-5-isothiocyanate
g	Gravity
g	Gram
h	Hour
HRP	Horseradish peroxidase
H_2O_2	Hydrogen peroxide
HuCRT	Human calreticulin
IgG	Immunoglobulin G
IWB	Immunowestern blot
kDa	Kilo Daltons
KO	Knock out
L/l	Liter
LDL	Low-Density Lipoprotein
LPS	Lipopolysaccharide
MHC	Major histocompatibility complex
M	Molar
mg	Milligram
min	Minutes
ml	Milliliter
mM	Millimolar
MmCRT	*Mus musculus* calreticulin
MoAb	Monoclonal antibody
MW	Molecular weight
µg	Microgram
µl	Microliter
µm	Micrometer
µM	Micromolar
Nº	Number
NBS	Neonate bovine serum
NBT	Nitrotetrazolium blue
ng	Nanogram
nm	Nanometer
PAGE	Polyacrylamide gel electrophoresis

PBS	Phosphate buffer saline
PCR	Polymerase chain reaction
PI	Post-infection
PSA	Ammonium persulphate
rTcCRT	Recombinant TcCRT
rHuCRT	Recombinant HuCRT
seg	Second
SDS	Sodium dodecyl sulphate
T. cruzi	*Trypanosoma cruzi*
TcCRT	*T. cruzi* calreticulin
TEM	Transmission electron microscopy
TEMED	N,N,N',N'-tetramethylethylenediamine
V	Volt
v	Volume
w	Weight
WCE	Whole cell extract

ABSTRACT

Trypanosoma cruzi calreticulin (TcCRT), a 47 kDa pleiotropic chaperone, besides its intracellular functional roles, is translocated from the endoplasmic reticulum (ER) to the area of flagellum emergence where it acts as a main virulence factor. Extracellular TcCRT mediates parasite infectivity by virtue of its capacity to interact with complement components C1 and MBL. Both inhibitions of the classical and lectin complement pathways are also consequences of these interactions. The localization and functions of TcCRT once the parasite is *inside* the host cell has not been reported. Herein we hypothesize that, during *T. cruzi* infection, and using specific antibodies, it is possible to detect TcCRT, once the parasite is *inside* the mammalian host cell. We also propose that TcCRT expression in the host cell inversely correlates with the MHC-I antigen expression. By experimentally addressing these issues we expect to contribute to the knowledge of the molecular terms governing the *T. cruzi*-host cell interplay, focusing on the role of TcCRT in particular *inside* the infected host cell. To reach this goal we will aim at validating the specificity of the antibodies to be used as TcCRT detector probes to identify TcCRT *inside* infected murine macrophages and, finally, to evaluate variations in surface MHC-I molecules on infected murine macrophages. Thus, we specifically and topographically monitor the TcCRT presence in parasites infecting a murine macrophage cell line, as compared to free trypomastigotes and non-infective epimastigotes. For that purpose, three different antibodies were tested as detector probes for immunocytochemical procedures. Polyclonal and monoclonal anti-TcCRT antibodies were validated as detector probes, as they showed minimal or null cross reactivity. In immunocytochemistry, polyclonal rabbit, and monoclonal murine anti-TcCRT antibodies, detected TcCRT with different sensitivities and specificities, when revealed with immune probes conjugated to colloidal gold, followed by transmission electron microscopy. With the rabbit polyclonal antibodies, CRT particles were observed, both in free parasites and infected host cells, mainly in the parasite nucleus and kinetoplast. With a murine monoclonal anti-TcCRT antibody, and using larger size gold particles, a drastic improvement in sensitivity and specificity for TcCRT detection, was obtained. TcCRT molecules were detected mainly in the trypomastigotes kinetoplast. We propose that this organelle may represent a stopover for TcCRT, generated in the ER, previous its translocation to the area of flagellum emergence. This mobilization may be influenced by the new

environmental conditions that the parasite meets *inside* the host cell. It remains to be determined the functional consequences of TcCRT cumulative presence in the kinetoplast. The possibility that TcCRT regulates transcription in kinetoplast DNA, as previously proposed for mammalian CRT in the nucleus, could be considered, although the DNA organization in the kinetoplast is different. Also, TcCRT may regulate Ca^{+2}-dependent transduction signalling pathways. Finally, by unknown mechanisms, *T. cruzi* infection seems to decrease the number of MHC class I positive cells, as early as 2h post-infection. It remains to be determined whether TcCRT accesses to the host cell ER and interferes in the MHC class I molecule-folding process.

RESUMEN

La calreticulina de *Trypanosoma cruzi* (TcCRT), una chaperona pleiotrópica de 47 kDa, se transloca desde el retículo endoplásmico (RE) a la zona de emergencia flagelar, donde actúa como un factor de virulencia principal, además de sus roles funcionales intracelulares. La TcCRT extracelular media la infectividad del parásito en virtud de su capacidad para interactuar con los componentes del complemento C1 y MBL. La inhibición de las vías del complemento clásica y de las lectinas también son consecuencias de estas interacciones. No se ha reportado respecto a la localización y funciones de TcCRT una vez que el parásito se encuentra en el interior de la célula hospedera. Aquí proponemos que, durante la infección por *T. cruzi*, y mediante el uso de anticuerpos específicos, es posible detectar TcCRT, una vez que el parásito se encuentra el interior de la célula hospedera de mamífero. También proponemos que la expresión de TcCRT en la célula hospedera se correlaciona inversamente con la expresión de antígenos MHC-I. Al abordar experimentalmente estos temas queremos contribuir al conocimiento de los términos moleculares que regulan la interacción células hospederas-*T.cruzi*, centrándose en el papel de TcCRT en particular, dentro de la célula hospedera infectada. Para alcanzar este objetivo apuntamos a la validación de la especificidad de los anticuerpos para ser utilizados como sondas detectoras de TcCRT, con ello identificar TcCRT interior de los macrófagos murinos infectados y, por último, evaluar las variaciones en la superficie de las moléculas de MHC- I en los macrófagos murinos infectados. Por lo tanto, específica y topográficamente se monitoreó la presencia de TcCRT en los parásitos que infectan a una línea celular de macrófagos murinos, en comparación con tripomastigotes libres y epimastigotes no infecciosos. Para ello, se probaron tres anticuerpos diferentes como sondas detectoras para procedimientos inmunocitoquímicos. Anticuerpos anti-TcCRT policlonales y monoclonales se validaron como sondas detectoras, ya que mostraron poca o nula reactividad cruzada. En inmunocitoquímica, el anticuerpo policlonal de conejo, y los anticuerpos monoclonales murinos anti-TcCRT, detectan TcCRT con diferentes sensibilidades y especificidades, cuando son revelados con inmunosondas conjugadas con oro coloidal, seguido por microscopía electrónica de transmisión. Con los anticuerpos policlonales de conejo, se observaron partículas de CRT, tanto en parásitos libres como en aquellos que se encuentran dentro del interior de células hospederas infectadas, principalmente en el núcleo y kinetoplasto del parásito. Con un anticuerpo monoclonal murino anti-TcCRT, y el uso de partículas de oro de tamaño más grande, se

obtuvo una mejora drástica en la sensibilidad y especificidad para la detección TcCRT. Se detectaron moléculas de TcCRT principalmente en el kinetoplasto del tripomastigote. Proponemos que este organelo puede representar una escala para TcCRT, generada en el RE, previo a su translocación a la zona de emergencia flagelar. Esta movilización puede estar influenciada por las nuevas condiciones ambientales con las que el parásito se encuentra en el interior de la célula hospedera. Queda por determinar las consecuencias funcionales de la presencia acumulada de TcCRT en el kinetoplasto. La posibilidad de que TcCRT regule la transcripción en el ADN del kinetoplasto, según lo propuesto anteriormente para la CRT de mamífero en el núcleo, podría ser considerada, aunque la organización de ADN en el kinetoplasto es diferente. Además, TcCRT podría regular vías de transducción de señales dependientes de Ca^{+2}. Finalmente, por mecanismos desconocidos, la infección por *T. cruzi* disminuye el número de células positivas MHC de clase I, tan temprano como 2 horas después de la infección. Queda por determinar si TcCRT accede al RE de la célula huésped e interfiere en el proceso de plegamiento de moléculas MHC clase I.

INTRODUCTION

1.- General Aspects

American Trypanosomiasis (Chagas' disease) currently affects over 10 million people, and the infection now spreads worldwide [1-3]. Its etiological agent is *Trypanosoma cruzi*, a hemoflagellate protozoan parasite that uses multiple strategies to evade the host immune system. Strategies to control Chagas' disease are oriented to the elimination of arthropod vectors, to the systematic control of blood donors in endemic countries, to the screening and treatment of children congenitally infected, among others.

There are currently 21 endemic countries, including Chile (about 150,000 cases), where annually 42,000 people become infected by vectors, 15,000 congenitally and 20,000 die. According to its chronicity, it is the parasitic disease with the greatest economic burden in America, mainly due to its productive impact on affected individuals. It has yet to be evaluated the impact of this parasitism in animal populations with economic or affective values, since they are susceptible to infection and act as parasite reservoirs.

Migration of infected people is a threat to public health in countries where there is no vector transmission, such as US, Canada and Spain (In US, however, was reported the vector transmission of the disease [4-6]). There, transmission is mainly through blood transfusions, organ transplantation [7] and congenital. Chile may be approaching to this scenario, since the vector transmission is relatively under control, but important migratory populations from neighbour countries may be contributing to keep the prevalence of the disease. In addition, infection by ingestion of food contaminated with the parasite is also important [8, 9].

Consequently, the control of this disease not only involves vectors, but also the elimination of the parasite in infected hosts (man and other mammals). The detailed knowledge of the mechanisms used by the parasite to evade the host immune system and its variety of virulence factors are key for the proper treatment of the disease.

In vertebrates, calreticulin (CRT) is an important, ER-resident lectin chaperone that, among many other pleiotropic functions, controls the proper folding and functions of a variety of proteins [10-13]. In *T. cruzi*, CRT (TcCRT), upon translocation from the ER to the area of flagellum emergence, mediates immune evasion strategies and acts as a relevant virulence factor [14-17] and antiangiogenic /anti-tumor moiety [18-20].

A large variety of pharmacologic and immunologic strategies are oriented to specifically interfere with virulence factors and parasite metabolic pathways [21-24]. However, secondary effects of current treatments [25-27] sustain the need to search for alternatives.

2.- American Trypanosomiasis [28]

American Trypanosomiasis or Chagas' disease was first described in 1907 by Dr. Carlos Chagas who detected a large number of patients with symptoms different to all described diseases. When analyzing the gut of hematophagous *Panstrongylus megistus,* discovered a parasite, *T. cruzi*, results that were published in 1909 [29].

2.1 *T. cruzi*

2.1.1 Biology:

T. cruzi is a hemoflagellate protozoan, with single flagellum and mitochondria (mitochondrion), where the kinetoplast, an organelle that contains specialized DNA, locates. *T. cruzi* has a fusiform flagellum, a microflagelar rod, subpellicular microtubules, glycosome (where part of glycolysis occurs) and a mitochondria-kinetoplast complex, among others. This protozoan has several cellular forms recognizable by light microscopy:

Trypomastigote: Around 25 μm long and 2 μm in diameter. The nucleus is located in the front and the kinetoplast to the posterior. The flagellum emerges from basal body near the kinetoplast and then folds forming an undulating membrane along the

parasite, emerging free at the other end and functioning as a driving flap. Trypomastigotes are found in the blood of the vertebrate host and in the gut, urine and faeces of the vector. This stage, although highly infectious, is not replicative.

Epimastigote: Between 20 and 40 μm long and 2 μm in diameter, with the kinetoplast located more centrally, above the nucleus. The flagellum arises again from the basal body, near the kinetoplast, forming a shorter membrane than the previous stadia, so they have less mobility than trypomastigotes. This stage is replicative and is observed in the gut of the vector insect or grown in axenic media.

Amastigote: With a short, non-emerging flagellum is a spherical form of the parasite, with the kinetoplast near the nucleus. It is commonly found inside host cells, where it replicates. It may also infect mammal cells [30].

The parasite is organized as follows:

a) CYTOSKELETON: One characteristic of *Trypanosomatidae* is the presence of a layer of microtubules located under the plasma membrane (also known as subpellicular microtubules). Microtubules are connected together and attached to the plasma membrane by short filaments of unknown nature. This association is likely responsible for the rigidity of the cell and its resistance to mechanical breakdown.

b) NUCLEUS: About 2.5 μm, elongated. In epimastigotes, is round. Its genome consists of 8.7 MB of DNA.

c) KINETOPLAST: As several members of the *Trypanosomatidae* family, *T. cruzi* has only a mitochondrion extending through the cell body. Near the basal body (organelle formed from a centriole, and a short cylindrical array of microtubules), there is a complex array of DNA fibrils in the mitochondrial matrix that forms the kinetoplast. About 1 μm long and 0.1 μm in depth, it is connected to the basal body by filamentous structures. It represents about 20-25% of the epimastigote DNA.

d) GLYCOSOMES: About 0.7 μm diameter. They are randomly distributed in the cell

with a slightly dense, homogeneous matrix in which most of the glycolytic pathway is located. They do not have detectable DNA.
e) CYTOSTOME: Funnel-shaped structure, located close to the flagellum emergence zone. This structure initially binds macromolecules like transferrin and LDL, which then are internalized through vesicles to the central portion of the parasite.

f) RESERVOSOMES: These organelles concentrate internalized macromolecules in the back of the cell. In this organelle, cruzipain, the most important cysteine protease of these parasites, accumulates.

g) ACIDOCALCISOMES: Vesicles with electron-dense content. Contains high concentrations of calcium ion and an ATPase activity dependent of the Ca^{+2}-H^{+} translocation.

2.1.2 Life Cycle:

Infective trypomastigotes enter the insect vector when it feeds from an infected mammal host. In the stomach of the insect, the trypomastigote transforms into an epimastigote, which replicates in the gut, and may adhere to intestinal cells of the insect. In the rectum, epimastigotes transforms into metacyclic trypomastigotes that are eliminated with faeces. These cellular forms are infective to the vertebrate host.

In the bloodstream, trypomastigotes penetrate *inside* host cells where they transform into amastigotes, which are replicative, intracellular forms. After several rounds of cell division, amastigotes transform back into trypomastigotes that are released into the extracellular space and from there into the bloodstream where they penetrate other cells, starting a new cycle (Fig.1).

This intracellular phase of the life cycle of *T. cruzi* is divided into different stages:

a) Adherence to the plasma membrane of the host cell.
b) Internalization of the trypomastigote into a phagosome.
c) Disruption and dispersion of the vacuolar (phagosome) membrane, thus releasing the parasites into the cytoplasm.

d) Multiplication in the host cell cytoplasm, as amastigotes.

e) Amastigotes transform back to trypomastigotes that can infect other host cells or infect the insect vector through its blood meal.

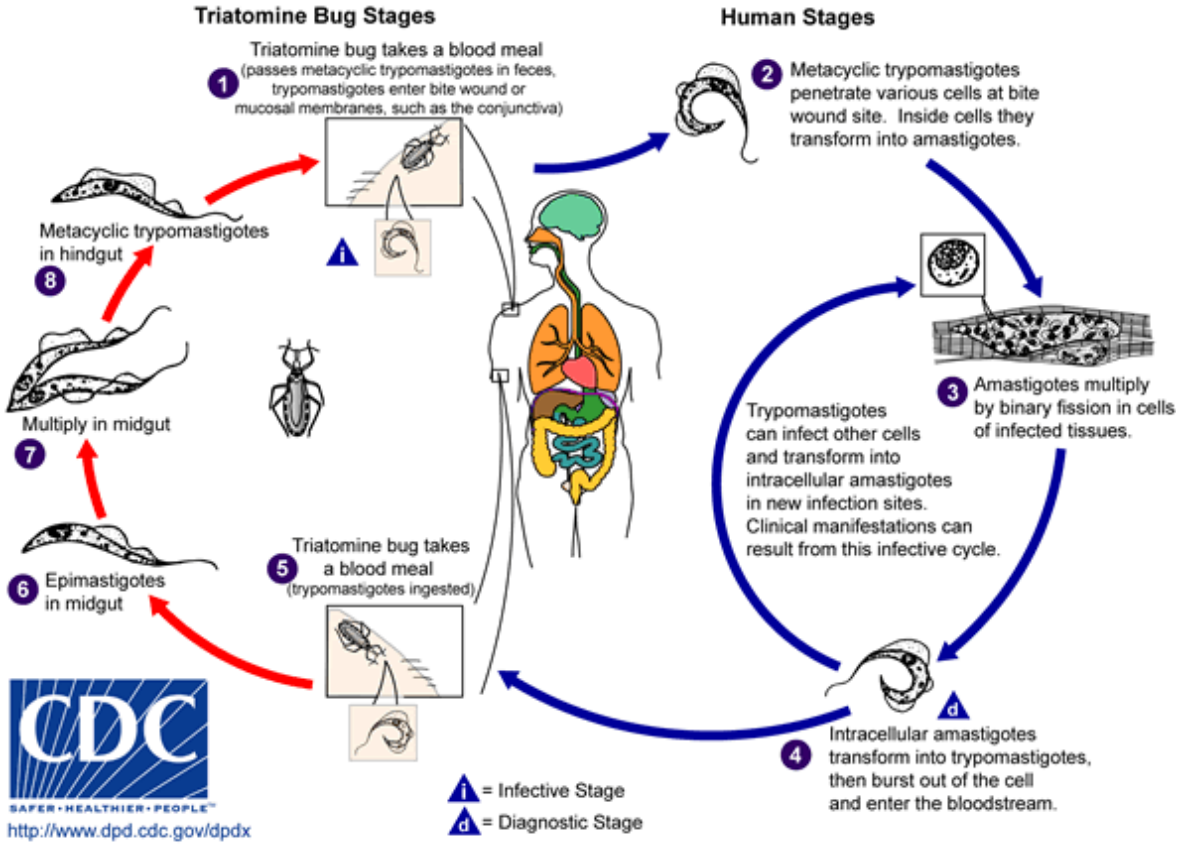

Figure 1: Life Cycle of *T. cruzi* [31].

Schematic representation of *T.cruzi* life cycle. In brief, from an infected mammal, the insect vector feeds with contaminated blood in which trypomastigotes are present. In the insect midgut, the trypomagtigotes differentiates into epimastigotes, a replicative form of the parasite. They differentiate into trypomastigotes that are eliminated through the faeces of the insect vector. In the bloodstream of a new infected mammal host, trypomastigotes penetrates inside mammal host cells, where they transform in amastigotes, which are replicative, intracellular forms. After several cell division cycles, amastigotes transform back into trypomastigotes that are released to the extracellular space.

3. - Calreticulin (CRT) from Vertebrates

CRT is a pleiotropic lectin-chaperone, involved in key functions in mammal cells [10, 13, 32]. Some basic considerations in regard to this protein are:

3.1 Structure:

CRT has 3 main domains: the N (amino terminal globular), the P (proline rich) and C (carboxy-terminal, where calcium ion binds with low affinity and high capacity). The N and P domains are highly conserved among species (Fig.2). CRT is located in the storage compartments associated with the ER, in the Golgi apparatus, and nucleus.

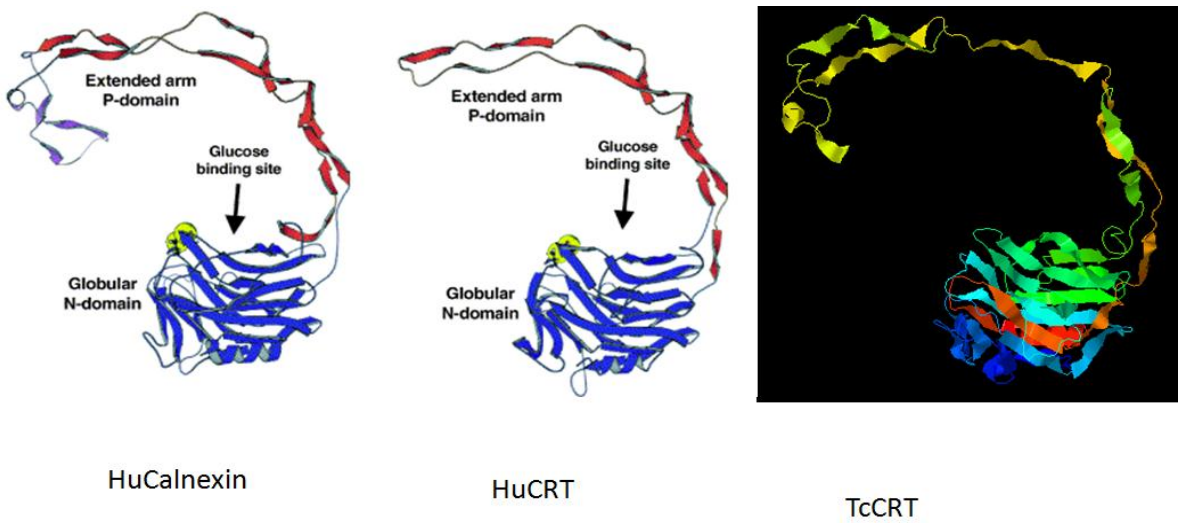

Figure 2: Proposed Model for Calnexin, TcCRT and HuCRT (courtesy of Dr. Gonzalo Cabrera, ICBM, Faculty of Medicine, University of Chile).

The TcCRT model was generated using the complete amino acid sequence of TcCRT. Two of its domains (Globular N-Domain, and part of the P-Domain) are represented in the figure. HuCRT and HuCalnexin models are added for comparison purposes.

3.2 Functions and Location:

CRT binds calcium with high capacity and low affinity through its carboxy-terminus domain [10, 13], thus regulating calcium storage and signalling [33]. Additionally, as a chaperone, it binds to oligosaccharides segments and prevents misfolded proteins to be exported from the ER to the Golgi [12]. Moreover, different mammalian species CRTs have ER retention signals in the carboxy-terminus domain [10, 34]. Together with calnexin, it stabilizes MHC-I molecules folding, consisting of a glycosylated H chain, β_2-microgobulin and the leader peptide. In this case, the emerging H chain joins calnexin, and then β_2 –microgobulin [11]. At this point, CRT becomes part of the peptide-loading complex. Evasion of immune recognition by virus, bacteria and parasites, includes, in many cases, disruption of this complex [35, 36], usually through retrograde transport mechanisms, which involve a KDEL receptor [37] such as *Pseudomonas* endotoxin A [38]. In CRT has also been described a retrograde transport mechanism, which would be independent of the conventional one employed for misfolded proteins [39].

CRT is also found in the nucleus, suggesting that it may play a role in the regulation of transcription. CRT binds to the synthetic peptide KLGFFKR, which is similar to an amino acid sequence of the DNA binding domain in the nuclear receptor super family. Its amino terminus interacts with the DNA binding domain of the glucocorticoid receptor and prevents binding to its specific response element (GRE). Therefore, it can act as an important modulator of the transcriptional regulation of genes regulated by nuclear hormone receptors genes [40-42].

Its vital importance is highlighted as *CRT* -/- KO mice die *in utero* 14 days post-fertilization [43]. Recently recognized extracellular functions of mammal CRT have been reviewed, such as a possible role in wound healing [44].

4.- Antigen Presentation [45, 46]

CRT has a key function in MHC-I protein folding. Related to this important role, what follows is an overview of the main mechanisms involved in antigen presentation.

4.1 Major Histocompatibility Complex (MHC) [46].

Located in the short arm of mouse chromosome 17, it contains numerous genes encoding proteins with a variety of immune functions, including MHC class I and II molecules.

i) MHC class I molecules: They present cytosolic intracellular peptides to $CD8^+$ T lymphocytes. They consist of two non-covalently linked polypeptide chains: the α, 44-47 kDa, and β_2-microgobulin, a 12 kDa molecule, that is encoded in a different part of the genome, that post-synthetically binds to the MHC-I α chain. This α chain has 3 domains, 2 forming the peptide-binding pocket (for peptides 8-11 amino acid long) and the third that binds to CD8 molecules on the cell. These molecules are expressed in all nucleated cells.

ii) MHC class II molecules: They present extracellular peptides in phagocytosed vesicles to $CD4^+$ T lymphocytes. Similar to MHC-I molecules, they consist of 2 polypeptide chains: α, 32-34 kDa, and β, 29-32 kDa, each having two domains. The α1 and β1 domains form the peptide-binding pocket (for peptides 10-30 amino acid long). The β2 domain binds CD4 molecules on the cell. Both chains are encoded in the MHC. A key role during the synthesis and trafficking of new molecules, and MHC-II peptides that bind it, is played by the invariant peptide. These molecules are preferentially expressed in antigen presenting cells.

4.2 MHC and Antigen Presentation to T cells [45]:

4.2.1 Antigen Presentation to $CD4^+$ Lymphocytes:

Most mammalian cells can endocytose and process protein antigens, but only a few can express MHC-II molecules, for example, dendritic cells, macrophages and B-lymphocytes.

For $CD4^+$ cell activation, an extracellular protein is internalized through endosomes, where it is degraded by enzymes that work at acidic pH. The newly synthesized MHC class II molecules, with the invariant peptide, are transported from

the ER to the endosome, where the invariant peptide is degraded and a small residuary fraction (CLIP) is removed from the peptide-binding pocket by the DM molecules (intracellular chaperones that works in lysosomes and endosomes). Finally, the peptides generated by the extracellular protein binds the MHC-II pocket region and the complex is exported to the cell surface. CRT has not been described to participate in the folding process of these molecules.

4.2.2 Antigen Presentation to $CD8^+$ Lymphocytes:

Unlike $CD4^+$ cells, any cell can present antigens to activate $CD8^+$ lymphocytes. In this case, a cytosolic protein is processed by the proteasome. The generated peptides are carried to the ER by a transporter (TAP), and then bind to MHC-I molecule. This complex (peptide – MHC-I) is transported to the Golgi, to finally form an exocytic vesicle that allows surface expression.

In this mechanism, the functions of chaperones calnexin and CRT are relevant, since during the process of biosynthesis of MHC-I molecules, they both monitor the correct folding and correct peptide loading in the pocket [11, 12]. The stages involved in MHC-I molecule folding process are presented in Fig. 3:

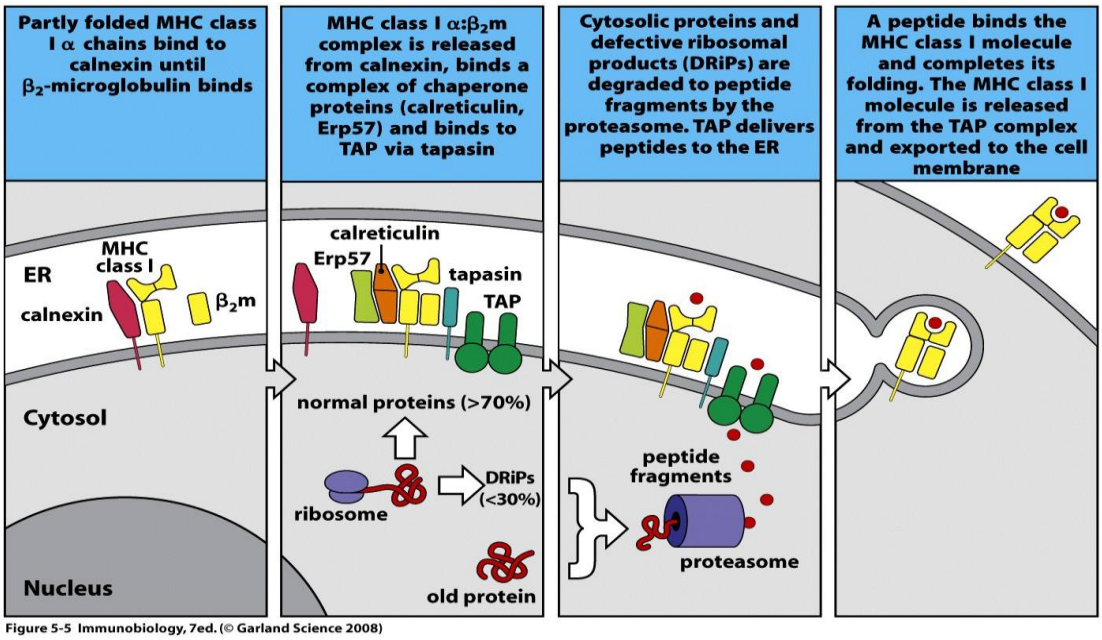

Figure 5-5 Immunobiology, 7ed. (© Garland Science 2008)

Figure 3: Schematic Representation of MHC-I Molecule Synthesis

MHC-I α chain assembles in the endoplasmic reticulum (ER) where is bound to calnexin. When the β_2-microgobulin (β_2m) post-synthetically binds to this complex, the dimmer α/β_2m dissociates from calnexin and then, the partially folded MHC-I molecule binds to the peptide transporter TAP by interacting with the TAP-associated protein, tapasin. The chaperones Erp57 and calreticulin also bind to form the peptide-loading complex. The MHC-I molecule is retained in the ER until released by binding of a peptide, which completes the MHC-I molecule folding.

5.- *T. cruzi* Calreticulin (TcCRT)

First described in 1991 [47], it is now recognized as a main virulence factor [17]. The localization of 4 main domains are presented in Fig.4:

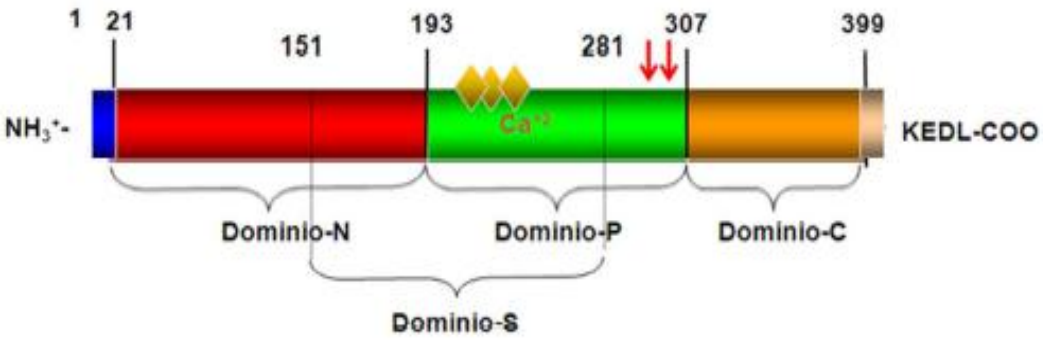

Figure 4: Schematic Representation of TcCRT [48]

A scheme of TcCRT principal domains is shown. They include the globular amino terminus, the proline-rich and the caboxy-terminus domains. Included in the diagram is the S domain, relevant in the interaction of TcCRT with complement components MBL and C1.

TcCRT is translocated from the ER to the flagellum emergence zone [15] (Fig.5) where, through its central S domain (amino acids 151-281) (Fig.4) interacts with C1, the first complement component, thus inhibiting the early stages of the classical pathway [15, 49]. Inactive C1 remains bound to the parasite mediating its interaction with host cell CRT, thus promoting infectivity [17].

The lectin complement pathway is also inhibited since TcCRT interacts with the mannan-binding lectin (MBL) and ficolins (Valck *et al*, Molec. Immunol. 2014, in press). Through a different domain, located in the amino terminal sequences, extracellular TcCRT interacts with endothelial cells, probably through a collagen-like Scavenger-receptor class A, since this interaction is inhibited by fucoidin, an homopolymer of sulfated L-fucose [18] (Abello *et al*, 2014, unpublished). TcCRT interaction with endotheliocytes results in antiangiogenic and antitumor effects. Additionally, in experimentally infected animals, TcCRT mediates autoimmune reactions focused on the heart [50]. Apparently, TcCRT performs all these properties in the extracellular space.

Faltan parámetros necesarios o son incorrectos.

On the other hand, monoallelic *TcCRT* KO parasites, the wild type, and a transgenic variant (with an extra *TcCRT* gene copy), display increasing survival capacity in the presence of human complement, as well as enhanced *in vivo* infectivity (*TcCRT* homozygous KO parasites are not viable) [51, 52]. TcCRT is located in different organelles, including the kinetoplast and the ER [53], even though this protein, as in mammals, has an ER retention signal [20]. This diverse localization allowed proposing a secretory pathway for TcCRT [53]. More recently, in vesicles secreted from the parasite to the extracellular milieu, TcCRT is among the proteins identified as part of the vesicle cargo [54].

6.- Main Issue Statement

Experimental evidence indicates that TcCRT, even though bearing an ER retention signal, is detected in several organelles, all consistent with a secretory pathway [53]. Moreover, in vesicles secreted from free parasites to the extracellular milieu, TcCRT is part of its protein cargo. Thus, TcCRT is translocated from the ER to the parasite flagellum emergence zone (Fig. 5), where vesicles can be found [53, 55]. The extracellular protein is involved in the infective process through its interaction with C1q [15] and modulation of the host complement system (classical and lectin pathways) among other important functions. All the former was studied in free parasites and the extracellular milieu.

TcCRT itinerary, when the parasite is *inside* the host cell, is not known. It is possible that TcCRT could be released from the trypomastigotes cytosol into the host cell cytoplasm, and then, the protein may access the ER if it avoids protein degradation in the proteasome. Once in the ER, and due to its high homology to mammalian CRT, it may compete for MHC-I molecules, and may interfere with the antigen presentation of the host cells. If so, a mechanism of immune evasion has yet to be described.

In synthesis:

a) The retrograde transport pathway, through which proteins destined to the ER return to the ER after been modified in the Golgi, is also a gateway for many viruses and toxins to access the ER. They partly accomplish this, by mimicking the ER retention signal, KDEL, at the carboxy-terminus domain and by escaping from the proteasome as no ubiquitination occurs, *i.e:* cholera toxin [35-37, 56].

b) Immunocytochemical localization studies with gold particles demonstrate that TcCRT is located in several organelles within the parasite, all of them consistent with a secretory pathway for TcCRT [53].

c) CRT is one of few proteins that retrotranslocates from the ER to the cytoplasm,

which would be independent of the mechanism used when misfolded proteins are destined for degradation [39].

d) The parasite can remain for years within the host, due to its ability to evade the host immune system. Among the mechanisms employed for that purpose, is the inhibition of peptide presentation (through MHC-II molecules) in infected macrophages. The molecule responsible for this inhibition was not identified at that time [57].

e) Given the importance of MHC-I peptide presentation to $CD8^+$ T lymphocytes in the control of *T. cruzi* infectivity, it is important to investigate whether this pathway of antigen presentation is altered with the infection.

f) If formation of the parasitophorous vacuole is inhibited, infectivity decreases [58].

g) Mammalian CRTs is about 50% identical and 80% homologous to TcCRT, been the amino-terminus domain the most conserved. TcCRT also possesses an ER retention signal (KEDL) homologous to the one present in mammalian CRT (KDEL) [48].

h) TcCRT cDNA is augmented during the first 24 h post-infection (PI) as detected by conventional PCR coupled to reverse transcriptase [17], which suggest increased protein synthesis during this period. As at 24 h PI amastigostes and trypomastigotes can be found in the host cell, the relative abundance of TcCRT cDNA for both stages of the parasite was compared, and no differences were observed, so the increase is not explained by the different stage.

Based on these rational elements, we propose the following hypotheses:

HYPOTHESES

During *T. cruzi* infection:

1. Using specific antibodies, it is possible to detect *T. cruzi* Calreticulin, once the parasite is *inside* the mammalian host cell.

2. TcCRT expression in the host cell inversely correlates with the expression of MHC-I molecules.

1.- General Aim

To contribute to the knowledge of the molecular terms governing the *T. cruzi*-host cell interplay, focusing on the role of parasite CRT in particular *inside* the infected host cell.

2.- Specific Aims

2.1 To validate the specificity of the antibodies to be used as TcCRT detector probes (Hypothesis I).

2.2 To detect TcCRT *inside* infected murine macrophages (Hypothesis I).

2.3 To evaluate variations in surface MHC-I molecules on infected murine macrophages (Hypothesis II).

MATERIALS AND METHODS

1.- Biological Material

1.1 Cell Lines

- Mouse leukaemic monocyte macrophages (RAW 264.7 cells) (Sigma-Aldrich, USA).

- African green monkey epithelial cells (VERO cells) were obtained from Institute of Public Health (Chile). They were cultured in RPMI medium supplemented with 10% v/v fetal bovine serum (FBS), 1% v/v penicillin/streptomycin and 1% v/v L-Glutamine to semi-confluence for further infection.

1.2 Parasites

- *T. cruzi* epimastigotes (Dm28c strain) were cultured in 80 ml of Diamond Medium (Tryptose, Tryptone and yeast extract, at 6.25 g/l each; 0.107 M NaCl, 0.03 M KH_2PO_4, 0.022 M K_2HPO_4, pH 7.2) supplemented with neonate bovine serum (NBS), Penicillin/Streptomycin, and Hemin, at 27ºC.

- *T. cruzi* trypomastigotes (Dm28c strain) were maintained in RPMI medium supplemented with 10% FBS v/v, 1% v/v penicillin/streptomycin and 1% v/v L-glutamine at 37ºC.

1.3 Recombinant and Endogenous Calreticulin

- rTcCRT: was generated as described [47]. In brief, *TcCRT* without its leader and its KEDL ER retention signals, was amplified by PCR and ligated to a pET-28b(+) vector. rTcCRT was expressed from *E. coli* BL21(DE3)pLysS, transformed with the pET-28b (+)/*TcCRT* plasmid. rTcCRT was purified by affinity chromatography.

- eTcCRT: was obtained as described [59]. In brief, eTcCRT was purified from epimastigote extract by affinity chromatography. Rabbit anti-TcCRT polyclonal antibodies were bound to cyanogen bromide activated sepharose column.

- rHuCRT: was generated similarly as rTcCRT. Cloned by Dr. Alexandre Gingras (Department of Infections, Immunity and Inflammation, University of Leicester, UK.) and expressed and purified in LIAM [50]. In brief, a *HuCRT* gene, coding for the residues 18-417, was amplified by PCR and ligated into the *Eco*RI/*Nde*I restriction sites of the pET-15b vector. rHuCRT was expressed from *E. coli* BL21(DE3)pLysS, transformed with the pET-15b (+)/*HuCRT* plasmid. rHuCRT was purified by affinity chromatography.

1.4 Polyclonal Antibodies (PoAb)

- Anti-TcCRT/Anti-TcS: A rabbit polyclonal antiserum was generated against rTcCRT or its functional S domain (TcS) [59]. Previous to the immunization, a pre-immune serum was obtained.

1.5 Monoclonal Anti-TcCRT E2G7 Antibody (MoAb)

A mouse monoclonal IgG1 anti-TcCRT antibody (MoAb E2G7) was generated against native purified TcCRT as described [60], using standard protocols [61]. MoAb purification from mouse ascites was performed by affinity chromatography.

2.- Reagents

- Abcam (UK): Goat anti-mouse IgG conjugated to 18 nm colloidal gold.
- BD Bioscience (USA): MoAb anti-$H2D^d$ conjugated to FITC.
- BioRad (USA): acrylamide, Bio-Rad Protein Assay, bis-acrylamide, ammonium persulphate, TEMED.
- Calbiochem (USA): protease inhibitor cocktail.
- Dako (USA): Goat anti-rabbit IgG conjugated to horseradish peroxidase (HRP), goat anti-rabbit IgG conjugated to alkaline phosphatase (AP), sheep anti-mouse IgG conjugated to AP.
- eBioscience (USA) : Mouse monoclonal IgG1 anti-HuCD45 (leukocyte common antigen).
- Electron Microscopy Science (USA): 200 MESH copper grids, 300 MESH nickel grids, kit EPON 812 epoxy resin, kit polybed epoxy resin, glutaraldehyde,

paraformaldehyde, lead citrate, uranyl acetate, osmium tetroxide, sodium cacodylate.

- GE-Healthcare (USA): Amersham hybond-ECL nitrocellulose membrane.
- Gibco (USA): L-glutamine, penicillin-streptomycin, trypsine.
- Hyclone (USA): Fetal bovine serum (FBS), RPMI medium,
- MERCK (GER): Hydrochloric acid, Bromophenol blue, sodium bicarbonate, sodium carbonate, sodium chloride, ethanol, sodium hydroxide, sodium azide, methanol.
- MP Biomedicals (USA): Micro-titration multi-well plate, 96-V shaped wells.
- New England Biolabs (USA): Colour-plus pre-stained protein marker, broad range.
- Novus Biologicals (USA): Polyclonal antibody anti-calreticulin.
- Sigma-Aldrich: (USA): BSA, Coomassie blue R250, 2-mercaptoethanol, NBT-BCIP, paraformaldehyde, SDS, Tris-base, Tween 20, Goat anti-rabbit IgG conjugated to 10 nm colloidal gold.
- Thermoscientific (USA): ABTS, 96 well-U shaped polystyrene microtiter plate.

3.- Methods

3.1 Validation of the Specificity of the Antibodies to be Used as TcCRT Detector Probes (Hypothesis I)

3.1.1 RAW 264.7 Whole Cell Extract (WCE) Preparation

RAW 264.7 murine macrophages were cultured in RPMI medium (Hyclone, USA) supplemented with 10% v/v FBS (Hyclone, USA), 1% v/v penicillin/streptomycin (Gibco, USA) and 1% v/v L-glutamine (Gibco, USA). $1x10^7$ cells were harvested, washed 3 times and pellet was resuspended in 1 ml of PBS (Sodium dihydrogen phosphate 0.0025 M, disodium hydrogen phosphate 0.02 M, sodium chloride 0.15 M, pH 7.2-7.4), 30 μl of Triton X-100 (Sigma, USA) and of protease inhibitor cocktail (Calbiochem, USA) were added to the cell preparation and mixture was placed on ice for 15 min Sonication of the mixture was performed for 20 sec at frequency Nº3 in Microson ultrasonic cell disruptor (Misonix, USA). A

final centrifugation of the extract was performed at 16,170 *g* for 25 min to remove any cell debris and supernatant was stored at -20ºC. Protein concentration was measured by Bradford [62].

3.1.2 Dm28c Epimastigotes WCE Preparation

Basically performed as described in 3.1. Epimastigotes were cultured in Diamond medium as described in 1.2. $5x10^7$ parasites were harvested to generate the extract.

3.1.3 SDS-PAGE

Three different conditions were performed: a) 10 ng of rTcCRT and 30 μg of RAW 264.7 WCE; b) 10 ng of rTcCRT, 300 ng of nTcCRT and 30 μg of RAW 264.7 and c) 30 μg of RAW 264.7, 30 μg of RAW 264.7 pre-incubated 15 min with 300 ng rTcCRT, 30 μg of epimastigote WCE and 30 μg of epimastigote WCE pre-incubated 15 min with 300 ng of rTcCRT. Each condition was separated through 12% polyacrylamide gel electrophoresis in Mini-Protean-2 chamber (BioRad, USA). Samples were heated at 100ºC in protein loading buffer 1x and then loaded in the gel. The electrophoresis ran at 100V and once finalized, the gel was transferred to a nitrocellulose membrane for IWB.

3.1.4 Immuno-Western Blot (IWB)

Previously separated proteins were transferred to nitrocellulose membranes, using a humid system, at 4ºC for 1h at 100V. Then, the membrane was blocked overnight at 4ºC in PBS with 5% w/v nonfat milk. The blocked membrane was incubated for 1.5h with anti-TcCRT, anti-TcS (different dilutions) or anti-MmCRT (1/1,000 v/v) PoAbs (see Methods section 1.4 and 2), or with E2G7 MoAb ($9.78x10^{-4}$ μg/μl, see Methods section 1.5) diluted in PBS with 3% w/v nonfat milk at room temperature. The membrane was washed 4 times with PBS, 0.05% v/v Tween 20 and then incubated with an anti-rabbit or anti-mouse IgG conjugated to AP, 1/1,000 v/v in PBS with 3% w/v nonfat milk for 1.5 h at room temperature. The membrane was washed and the enzymatic reaction mediated by the antibody union was detected with NBT-BCIP.

3.1.5 Indirect Enzyme-linked Immunosorbent Assay (ELISA)

Microtiter plates were sensitized with 100 µl of MoAb E2G7 or anti-HuCD45 (isotype negative control) 5 µg/ml per well in carbonate buffer (sodium carbonate decahydrate 8.4 g/l, sodium bicarbonate 3.56 g/l) at 4ºC. Non-reactive sites were blocked with 5% w/v BSA in PBS for 2h at 37ºC. Plates were washed 4 times with PBS-0.05% v/v Tween, and then 100 µl of rTcCRT 1.25 µg/ml was added per plate and incubated for 2h at 37ºC. rHuCRT was used as antigen control. In a second plate, 10 µg/ml of epimastigote or RAW 264.7 WCE was added as antigen source. The same extracts pre-incubated for 15 min with rTcCRT 1 µg/ml were also evaluated. After washing, polyclonal anti-TcCRT antibody 1/5,000 v/v was incubated for 1.5h at 37ºC. Pre-immune serum was used as control. A secondary anti rabbit-IgG conjugated to peroxidase 1/1,000 was incubated for 1.5h at 37ºC, after washing with PBS-0.05% v/v Tween. Finally, after a wash with PBS-0.05% v/v Tween 20, 100 µl per well of ABTS-30% v/v H_2O_2 were added and plates were read at 405 nm.

3.2 Detection of TcCRT *inside* Infected Murine Macrophages (Hypothesis I)

3.2.1 Transmission Electron Microscopy (TEM)

3.2.1.1 Cell Culture

Murine macrophages (RAW 264.7, $5x10^6$ cells) were infected with $5x10^7$ trypomastigotes (Dm28c strain). Cell culture was performed in RPMI medium supplemented with 10% v/v FBS, 1% v/v penicillin/streptomycin and 1% v/v L-glutamine, at 37ºC. Cells were harvested at 2, 4 and 6h PI, and processed for TEM. As control, $5x10^6$ non-infected macrophages were harvested simultaneously. For comparison purposes, $1.5x10^8$ trypomastigotes and epimastigotes were obtained and processed for Immunocytochemistry.

3.2.1.2 TEM

Infected and non-infected cells were harvested, washed twice with PBS 1x, fixed in 3% v/v glutaraldehyde, overnight at 4ºC, washed and post-fixed with 1% v/v osmium tetroxide in phosphate buffer (sodium phosphate 0.1 M, pH 7.3). Samples were rinsed and progressively dehydrated in ethanol from 30% to absolute degrees, treated with acetone and finally embedded in EPON at 70ºC. Ultrathin sections (700 Aº), were placed on copper grids, stained with 5% w/v aqueous uranyl acetate and 0.04% w/v lead citrate and then observed at 80 kV in Zeiss EM-109 electron microscope (Carl Zeiss, GER).

3.2.1.3 Immunocytochemistry

Performed as previously described [53] with some modifications. Cells and parasites were fixed in 4% v/v paraformaldehyde and 0.1% v/v glutaraldehyde in cacodylate buffer (sodium cacodylate 0.1M, pH 7.2) o.n at 4ºC. Free aldehyde groups were blocked with 50 mM ammonium chloride. Samples were rinsed and sequentially dehydrated in 30% to absolute ethanol, at room temperature and embedded in polybed at 60ºC. Ultrathin sections of 700 Aº were obtained, collected on nickel grids, and, after immunocytochemical procedures, were stained with 5% w/v aqueous uranyl acetate, and then observed at 80 kV in Zeiss EM-109 and in Phillips-TECNAI 12 (Phillips, NLD) electron microscopes.

3.2.1.4 Immunocytochemical Procedures for CRT Detection

Nickel grids containing sections of 700 Aº were floated, for 30 min at room temperature, in Bufi (0.02M Tris, pH 7.2, 0.02% w/v sodium azide, 0.15 M sodium chloride, 0.1% w/v BSA, 0.05% v/v Triton X-100). Then, the sections were incubated overnight at 4ºC with a primary antibody (Polyclonal anti-rTcCRT 1/32,000 v/v, anti-MmCRT 1/100 v/v or monoclonal E2G7 anti-TcCRT 0.00489 μg/μl) diluted in BuFi. After washing in BuFi, sections were incubated for 2h with a

secondary antibody (goat anti-rabbit IgG conjugated to 10 nm diameter colloidal gold, or goat anti-mouse IgG conjugated to 18 nm diameter colloidal gold) diluted 1/20 v/v in BuFi, prior centrifugation for 10 min at 2,000 *g*. After washing, the sections were rinsed with deionized water. Controls include sections incubated with secondary antibody, pre-immune serum, and isotype control (IgG1).

3.2.2 Quantification of Label Density Generated by Polyclonal Antibodies

Gold particles/μm^2 in different compartments of the host cell were quantified using Image Analysis Routines (SCIAN-Soft) based on Interactive Data Language IDL 7.1 (ITT, Boulder, CO). For statistical analysis, the compartments of 4 different cells per condition were analyzed.

3.2.3 Quantification of Gold Particles in Kinetoplast Sections

Since 18 nm gold particles are easily resolved, their numbers in kinetoplast sections, obtained from different parasite stages, were quantified by their direct observation on the TEM photographs located under a transparent film. Each gold particle was counted out by labelling it on the transparent film, using a marker. Each photo was counted 3 times, and the average value of minimum 5 photos per condition was used for statistical analysis.

3.3 Evaluation of Variations in Surface MHC-I Molecules on Infected Murine Macrophages (Hypothesis II)

3.3.1 Flow Cytometry Procedure

RAW cells ($5x10^5$) were infected for 2, 4 and 6h with $5x10^6$ trypomastigotes (Dm28c strain), each condition in triplicate. Non-infected RAW 264.7 cells ($5x10^5$) were used as control. Cells were washed twice in PBS 1x (380 *g* for 5 min each), placed on a V- bottom microtiter plate, incubated with 100 µl of MoAb anti-$H2D^d$, conjugated to FITC (1/50 v/v), per well, 30 min in darkness. Samples were washed twice with PBS 1x, fixed with 1% v/v paraformaldehyde, 100 µl per well, 30 min at 4ºC and stored at 4ºC until data analysis.

3.3.2 Data Analysis

Data were obtained in FACSCalibur-4 colour flow cytometer (Becton Dickinson, 2007) and were analyzed with the program FlowJo 8.7, Mackintosh version, Tree Star Incorporated.

3.4 Statistical Analysis

The number of gold particles (see methods 3.2.2-3.2.3) and MHC-I positive cells (see methods 3.3.1) were statistically validated using one and/or two-way ANOVA tests, which were performed with Graphpad Prism 5.0, Macintosh version, Software Mackiev, Graphpad software Inc.

4.- Services

Electron microscopy sample processing and grids preparation were performed in the CESAT Unit, Electron Microscopy Laboratory, Faculty of Medicine, University of Chile.

Electron microscopy photographs were obtained in CESAT Unit, Electron Microscopy Laboratory, Faculty of Medicine, University of Chile, and in Advanced Electron Microscopy Unit, Faculty of Biological Sciences, Pontifical Catholic University of Chile.

RESULTS

1.- Validation of the Specificity of the Antibodies to be Used as TcCRT Detector Probes (Hypothesis I)

For the development of this Thesis, it was first necessary to standardize sensitive and specific means to detect TcCRT once the parasite is *inside* infected murine macrophages. Several antibodies were tested by IWB to select the most appropriate one to be used as detector probe in Immunocytochemistry, as described below.

1.1 IWB

Several antibodies anti-TcCRT (or its domains) were available as detector probes. In this case, we focused on two sets of polyclonal antibodies (PoAbs).

- **Detection with Anti-TcCRT PoAbs**

In the Methods Section, generation of a WCE of RAW 264.7 was described (see Methods Section 3.1). 30 μg of this extract, which is used as a source of MmCRT, was transferred to a nitrocellulose membrane and incubated with several different dilutions of the anti-TcCRT PoAb. In RAW 264.7 WCE a 58-kDa immunoreactive band was detected in several dilutions of the anti-TcCRT polyclonal serum, up until a dilution of 1/4,000 v/v (Fig. 6). In the three last dilutions tested no cross-reactivity was observed, which suggest that this antibody could be suitable to be used as detector probe in Immunocytochemistry, at high dilutions to minimize the cross-reactivity.

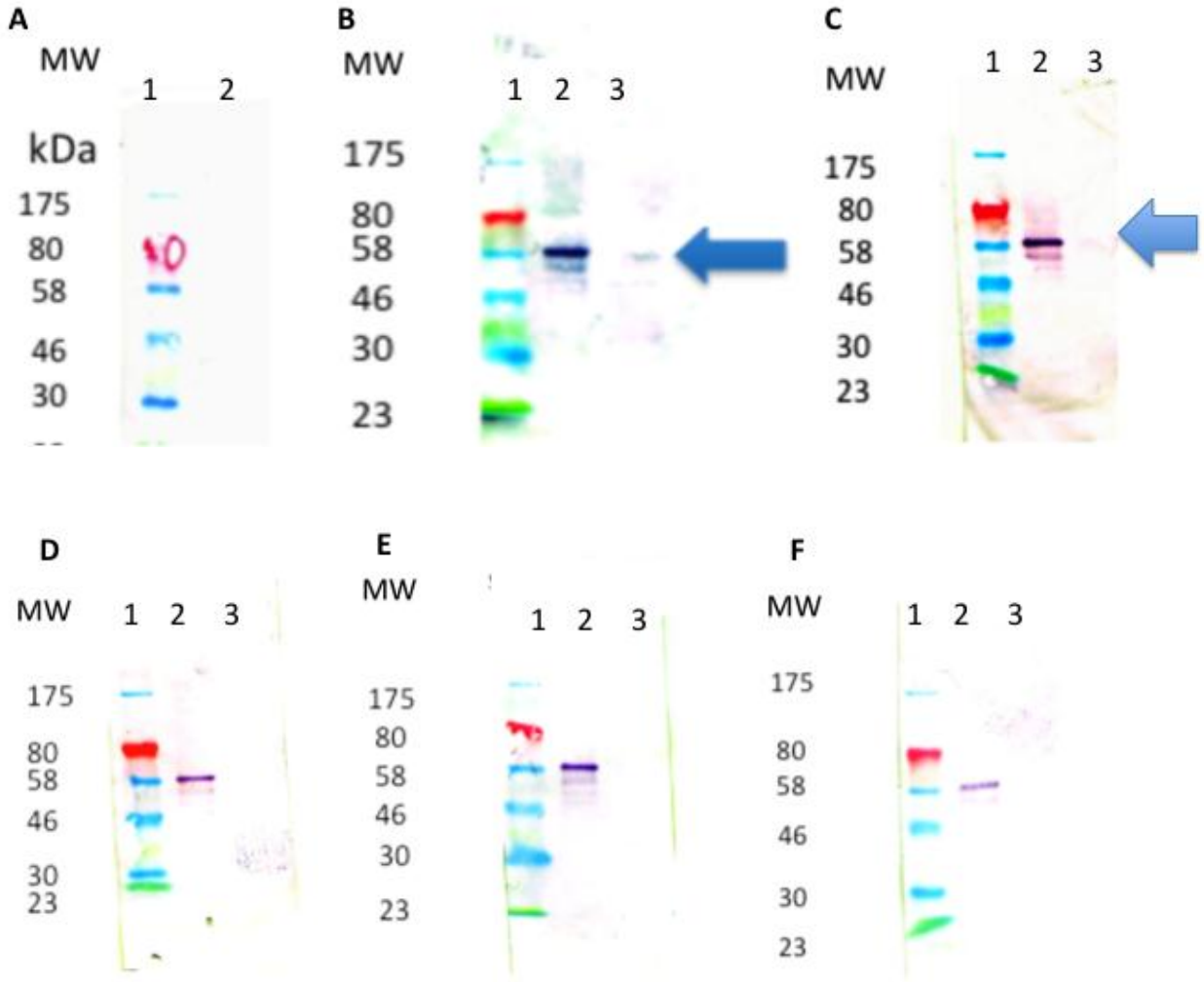

Figure 6: A Polyclonal Anti-TcCRT Serum Detects a 58 kDa Molecule, Antigenically Homologous with MmCRT.

A 58 kDa molecule is detected by cross reactivity at low dilutions of the antibody. **A:** Pre-immune serum 1/1000 v/v. Samples incubated with anti-TcCRT PoAb diluted v/v: **B:** 1/1,000, **C:** 1/2,000, **D:** 1/4,000**, E:** 1/8,000, **F:** 1/16,000.

A: lane 1: Molecular weight standard, lane 2: rTcCRT.

B-F: lane 1: Molecular weight standard, lane 2: rTcCRT, lane 3: RAW 264.7 WCE.

Arrows: 58 kDa putative MmCRT.

- **Detection with Anti-TcS PoAbs**

Since there was cross-reactivity with the anti-TcCRT polyclonal serum, another serum, generated against the TcCRT S domain (TcS, amino acids 159-281) was also tested as an alternative.

In this case, a 46 kDa immunoreactive band was detected in all dilutions employed in RAW 264.7 WCE, and at low dilutions, a slight band of 58 kDa was observed (Fig.23). Since this molecular weight does not correspond to conventional MmCRT, we cannot rule out the presence of a non-described MmCRT isoform, as in the *Mus musculus* genome two *crt* genes were detected [63]. The 58 kDa molecule is poorly detected, in part, as this antibody was generated with the recombinant S Domain, and not rTcCRT.

Given the specificity of the recognition of the 46 kDa molecule, we decided to further study this protein. The results are summarized in ANNEX I, since this subject somehow escapes from the Hypotheses context and this antibody was not employed in immunocytochemistry analysis.

- **Detection with Homologous Anti-MmCRT PoAbs**

In order to corroborate previous results, RAW 264.7 WCE was tested with the respective anti-MmCRT polyclonal antibody. A slight band of 58 kDa was observed, consistent with the band detected by the anti-TcCRT polyclonal serum (Fig.7).

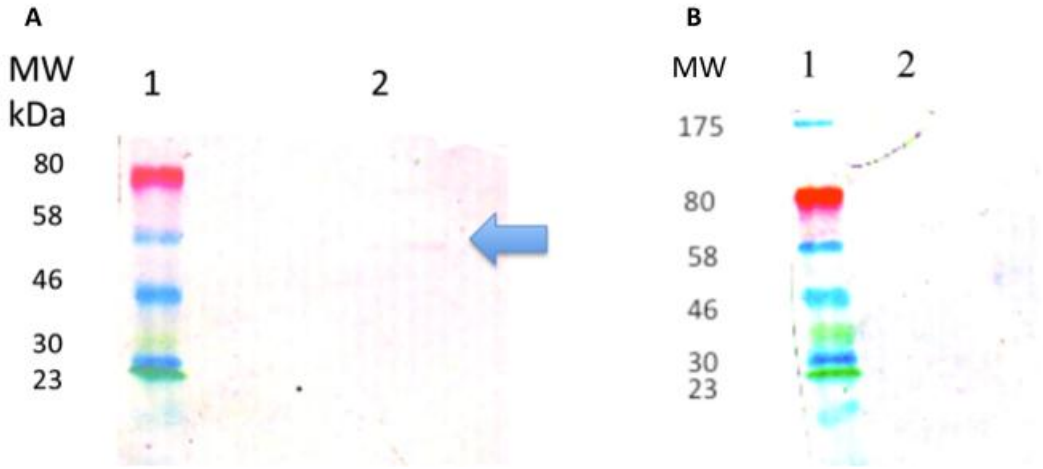

Figure 7: A Polyclonal Anti-MmCRT Serum Detects MmCRT in RAW 264.7 WCE.

Concordant to previous results (Fig.6) an homologous anti-MmCRT PoAb detects a 58 kDa MmCRT.

A: Anti-MmCRT PoAb diluted 1/1,000 v/v, **B:** Pre-immune serum diluted 1/1,000 v/v.

A-B: Lane 1: Molecular weight standard, Lane 2: RAW 264.7 WCE. Arrow: 58 kDa MmCRT.

- **Detection with Anti-TcCRT Monoclonal Antibody**

As an alternative to the anti-TcCRT polyclonal serum, a mouse IgG1 MoAb E2G7 anti-TcCRT was tested as possible detector probe. It detected rTcCRT and eTcCRT in different contexts, either purified (rTcCRT and eTcCRT) or direct from an epimastigote WCE (Fig.8A). When both extracts were employed as source of antigen, in RAW 264.7 WCE there was no detectable cross-reactivity. In epimastigotes extract, there was detection of eTcCRT. When both extracts were pre-incubated for 15 min with rTcCRT, the detection of the recombinant molecule was predominant in both cases, with the characteristic banding of rTcCRT. This molecule is less stable than eTcCRT, which was demonstrated by previous results, thus is more susceptible to degradation. rTcCRT is partially proteolyzed during the extract/IWB process when it was pre-incubated with the RAW 264.7 WCE, which could explain, in part, the differences obtained when the epimastigote WCE was pre-incubated with the recombinant molecule (Fig.8B). A pre-immune serum was employed as control, since at the time of the experiment no proper isotype control was available (Fig. 8C).

1.2 Indirect Enzyme-linked Immunosorbent Assay (ELISA)

In order to validate the E2G7 MoAb with the antigen in a more physiological way, closer to what it would be in Immunocytochemistry, an indirect ELISA was performed.

First, the specificity of the antibody was validated as rTcCRT was specifically captured by the E2G7 MoAb when compared to several controls (Fig.9A). When RAW 264.7 or epimastigotes WCE were employed as source of antigen, no CRT (eTcCRT or MmCRT) was captured, probably due to the low concentration present in the extracts. When both extracts were pre-incubated with rTcCRT, the recombinant molecule was effectively captured by the E2G7 MoAb (Fig.9B), which indicates that in this physiological approach, rTcCRT does not interact with other proteins through the epitope recognized by the E2G7 MoAb.

Taken together with the previous IWB results, this antibody is also a candidate to be employed as detector probe in immunocytochemistry.

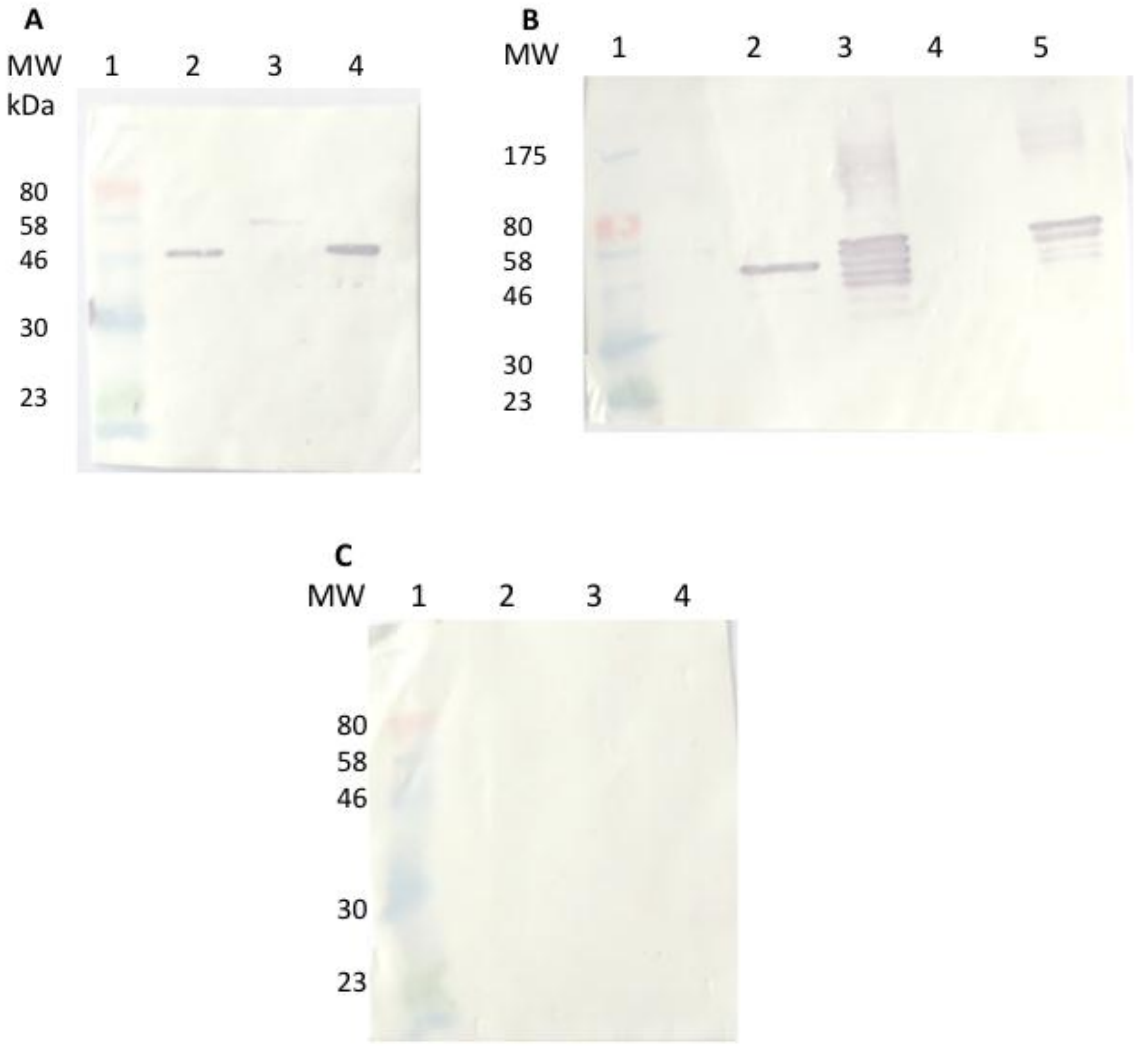

Figure 8: A E2G7 Anti-TcCRT MoAb Detects eTcCRT and rTCRT in Different Conditions.

rTcCRT and eTcCRT were detected either purified or from a direct epimastigotes WCE (eTcCRT). When RAW 264.7 WCE was employed as antigen source, no molecule was detected. Only when extract was preincubated with rTcCRT, the recombinant protein was detected.

A-B: E2G7 MoAb 9.78×10^{-4} μg/μl, **C:** Pre-immune serum 1/500 v/v ***.**

A,C: Lane 1: Molecular weight standard, lane 2: eTcCRT, Lane 3: rTcCRT, lane 4: Epimastigote WCE.

B: lane 1: Molecular weight standard, lane 2: Epimastigote WCE, lane 3: Epimastigote WCE + rTcCRT, lane 4: RAW 264.7 WCE, lane 5: RAW 264.7 WCE + rTcCRT.

*At the time of this experiment, no appropriate isotype control was available.

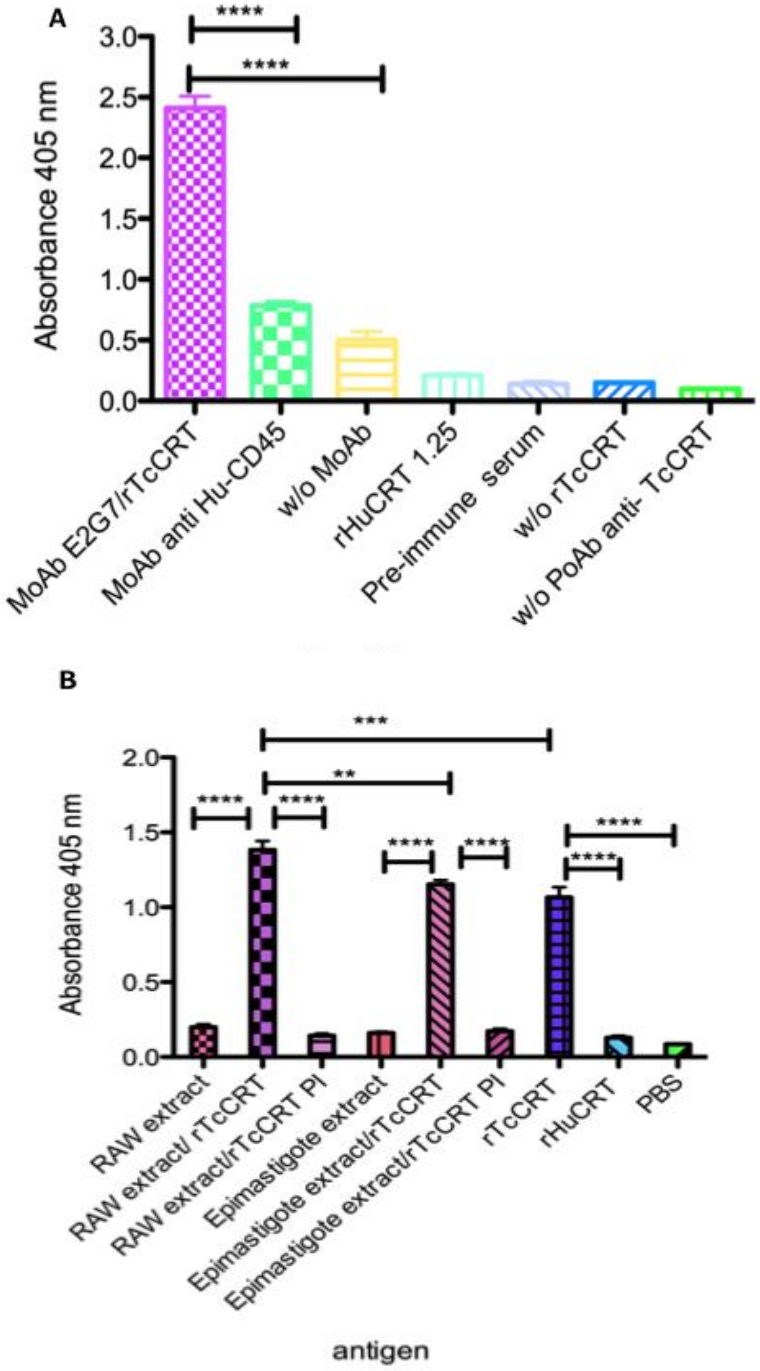

Figure 9: A E2G7 Anti-TcCRT MoAb Specifically Captures rTcCRT.

rTcCRT is specifically captured by the E2G7 MoAb, as compared to several controls (**A**). No CRT is captured when RAW 264.7 or epimastigotes WCEs are used as source of antigen. Only pre-incubation with rTcCRT allows positive signal of TcCRT capture. rTcCRT was employed as positive control, and rHuCRT as negative control (**B**).

A-B: Indirect ELISA. One-way ANOVA analysis, ****: p< 0.0001, ***: p<0.001, **: p<0.01. Bars: Standard deviation.

2.- Detection of TcCRT *inside* Infected Murine Macrophages (Hypothesis I)

2.1 Transmission Electron Microscopy

- **Organelle and Parasite Distribution in Infected and Non-Infected Cells**

In order to have a proper topographic control, the murine macrophage cell line RAW 264.7 was infected with trypomastigotes (Dm28c strain), as described in the Methods Section. Sections of infected and non-infected cells were processed for TEM. Resolution seems adequate since ribosomes can be observed in non-infected RAW cells (Fig.10A). At 2 and 4h post-infection (PI) (Figs.10B-10C), parasites can be observed inside the parasitophorous vacuole and, at 6h PI, parasites are also found free in the host cell cytoplasm (Fig.10D). Multiple vacuoles are seen at 4h PI (Fig.10C).

- **Calreticulin is Detected by Polyclonal Rabbit Antibodies, in Infected Cells**

Once the appropriate dilution was established, the immunocytochemistry procedures were performed. In non-infected macrophages, gold particles are detected when the corresponding anti-MmCRT PoAb was employed, especially in nucleus (nuclear heterochromatin) and cytoplasm (Fig.11). The 10 nm gold-particles are properly resolved in this microscope, indicating that the resolution is appropriate.

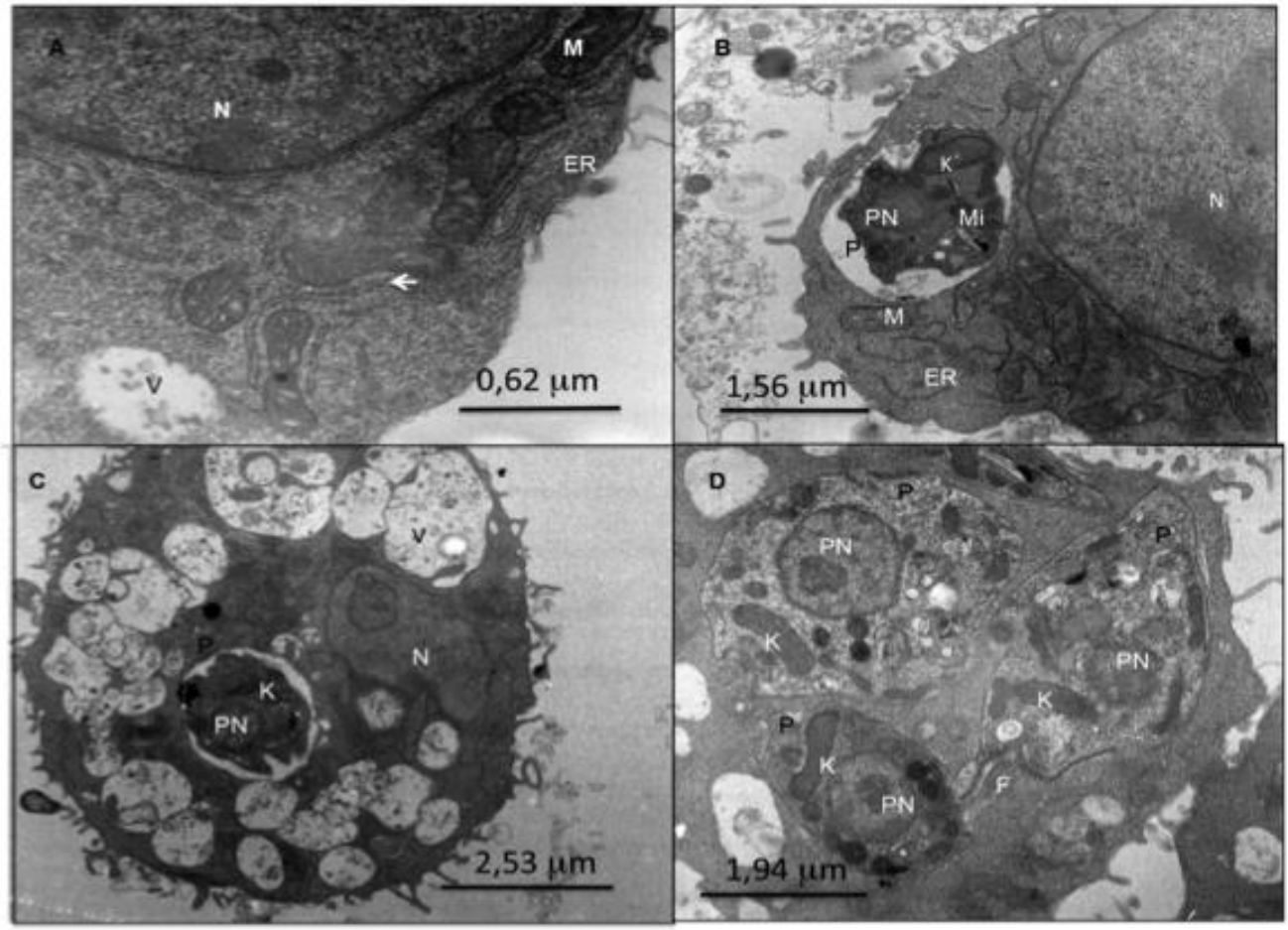

Figure 10: Host Cell and Parasite Organelles are Resolved by Electron Microscopy in Infected Macrophages

Electron microphotographs of infected and non-infected murine macrophages are shown **A:** In a non-infected cell (30,000x), ribosomes are resolved (arrow). Parasite sections (P) are shown inside macrophages at different hours post-infection. **B:** Inside a parasitophorous vacuole, at 2h (20,000x); **C:** At 4h (7,000x), in a vacuolated host cell and **D:** At 6h (12,000x), 3 parasite sections are observed free in the cytoplasm.

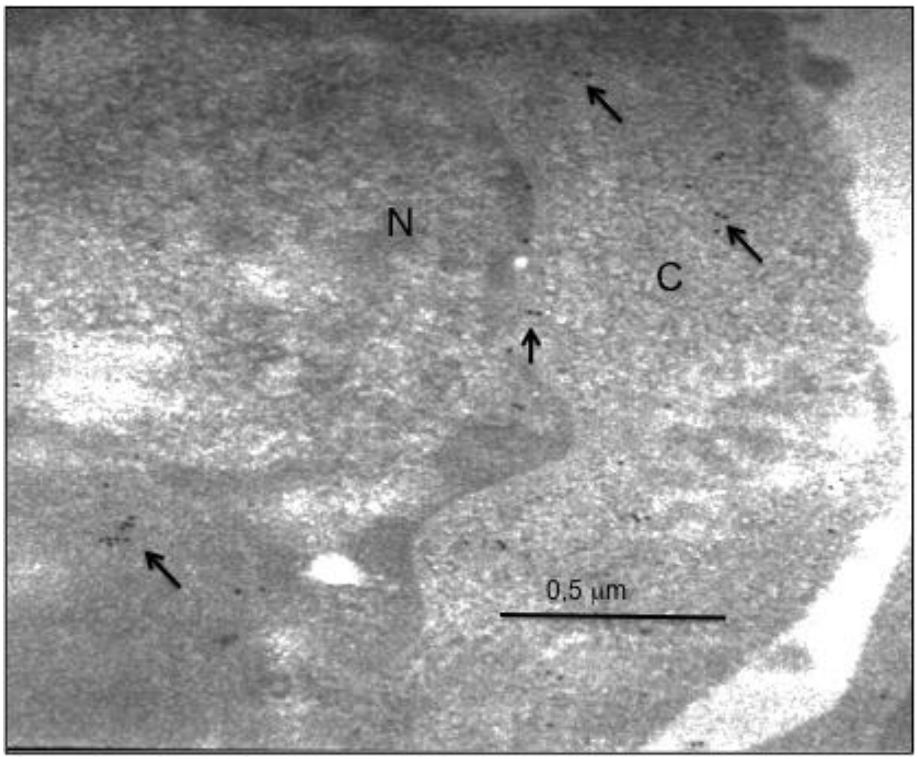

Figure 11: Host Cell Calreticulin is Detected with Homologous Polyclonal Antibodies.

Electron microphotograph of a non-infected murine macrophage is shown. Few gold particles were observed in nucleus (N) and cytoplasm (C) (arrows). Anti-MmCRT 1/100 v/v. Electron microphotograph was obtained at 30,000x.

Once the resolution of the microscope was shown to be adequate, as observed with the homologous anti-MmCRT PoAb, the first of the two antibodies validated as detector probes was employed.

Using the anti-TcCRT PoAb, some gold particles can be observed in the non-infected murine macrophage, which could correspond to background reactivity with MmCRT. Some particles were observed in nucleus, cytoplasm, and, as expected, in the ER (Fig.12A). In free epimastigotes, as expected [53], the label was observed basically in nucleus (Fig.12B). In agreement with previous results [53] in free trypomastigotes (Fig.12C), gold particles were observed in the kinetoplast, and a unidirectional flow towards the flagellum emergence zone can be proposed. Also, as expected [53], particles are found in vesicles near (or emerging) from the trypomastigote.

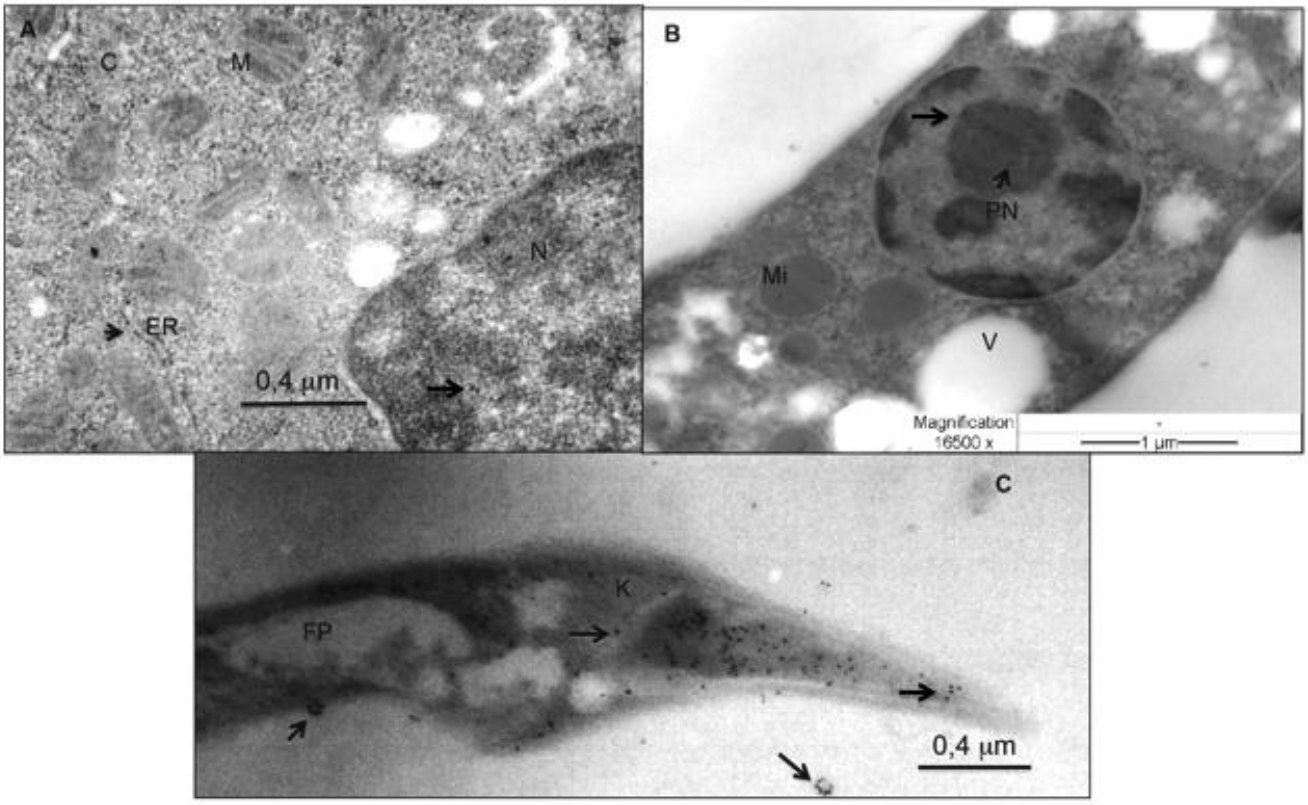

Figure 12: Calreticulin is Detected in Free Parasites and in Non-Infected Host Cell Organelles

Electron microphotographs of a non-infected cell and free parasites are shown. Gold particles are observed in: **A.** A non-infected cell (30,000x), in the nucleus (N), cytoplasm (C), and the endoplasmic reticulum (ER). **B.** A free epimastigote (16,500x), in the nucleus (N). **C.** A free trypomastigote (30,000X), in the kinetoplast and the flagellum emergence zone, as well as in vesicle-like structures (arrows). In host cell: ER: Endoplasmic reticulum, M: Mitochondria, N: Nucleus, C: Cytoplasm. In parasites: K: Kinetoplast, FP: Flagellum pocket, V: Vacuole, Mi: Mitochondrion, PN: Parasite nucleus. Arrows: Positive signals.

On infected cells, at 2h PI, gold particles were observed in the parasitophorous vacuole, and in the host cell cytoplasm. In the parasite, nucleus and kinetoplast are among the organelles where a high-density label can be observed. Interestingly, there was a label concentration on structures similar to those observed in free trypomastigotes, *inside* the parasitophorous vacuole (*outside* the parasite), in the borderline of the parasitophorous vacuole, and in the host cell cytoplasm (Fig.13A).

At 4h PI, a parasite was observed outside the host cell, presumably before being phagocytosed. Gold particles were detected in several organelles in the parasite, but more condensed in nucleus and kinetoplast. In the host cell, gold particles are observed in the cytoplasm and nucleus (Fig.13B).

At 6h PI, gold particles were observed in the parasitophorous vacuole, as expected, nucleus and kinetoplast among the organelles with more label concentration. In the host cell, gold particles were observed at the nucleus and cytoplasm (Fig.13C). As observed previously (Fig.12C, Fig.13A), there was concentration of the label on structures similar to vesicles on the edge of the parasitophorous vacuole. These structures are consistent with those previously described [54].

No gold particles were observed in 6h PI samples incubated with just the secondary gold- labelled antibody (Fig.13D) or with pre-immune sera (Fig.13E), suggesting specific labelling.

An amplification of a parasite inside a parasitophorous vacuole at 2h PI (Fig.14) showed the presence of vesicle-like structures, similar to those observed in free trypomastigotes (Fig.12C).

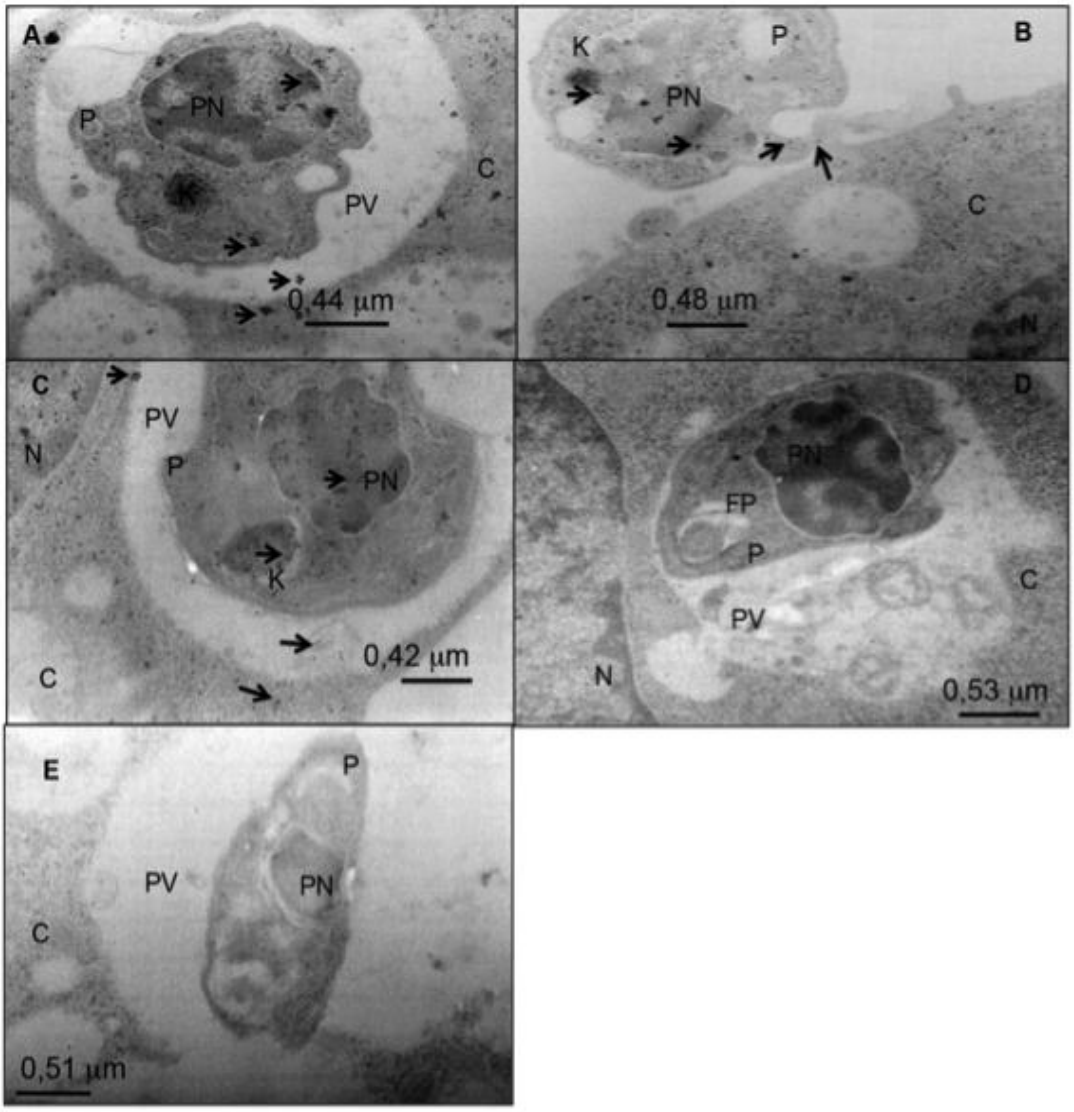

Figure 13: Calreticulin is Detected by Rabbit Polyclonal Antibodies in Infected Macrophages

After infection, gold particles were detected at: **A.** 2h, in the parasite nucleus and kinetoplast, in the host cell cytoplasm and in vesicle-like structures (arrows); **B.** 4h, in a parasite outside the host cell, mainly in the parasite nucleus and kinetoplast; Also, in the murine macrophage nucleus and cytoplasm; **C:** 6h, mainly in the parasite nucleus and kinetoplast, and in vesicle-like structure in the host cell cytoplasm (arrow); **D-E:** 6h, control samples. No gold particles were observed.

A-C: Anti-rTcCRT polyclonal serum, 1/32,000 v/v; **D:** Anti-rabbit IgG conjugated to colloidal gold (10 nm), 1/20 v/v; **E:** Pre-immune serum 1/32,000 v/v.

In host cell: N: Nucleus, C: Cytoplasm, PV: Parasitophorous vacuole. In parasites: P: Parasite, K: Kinetoplast, FP: Flagellum pocket, V: Vacuole, Mi: Mitochondrion, PN: Parasite nucleus. Arrows: Positive signals. All samples are 30,000x.

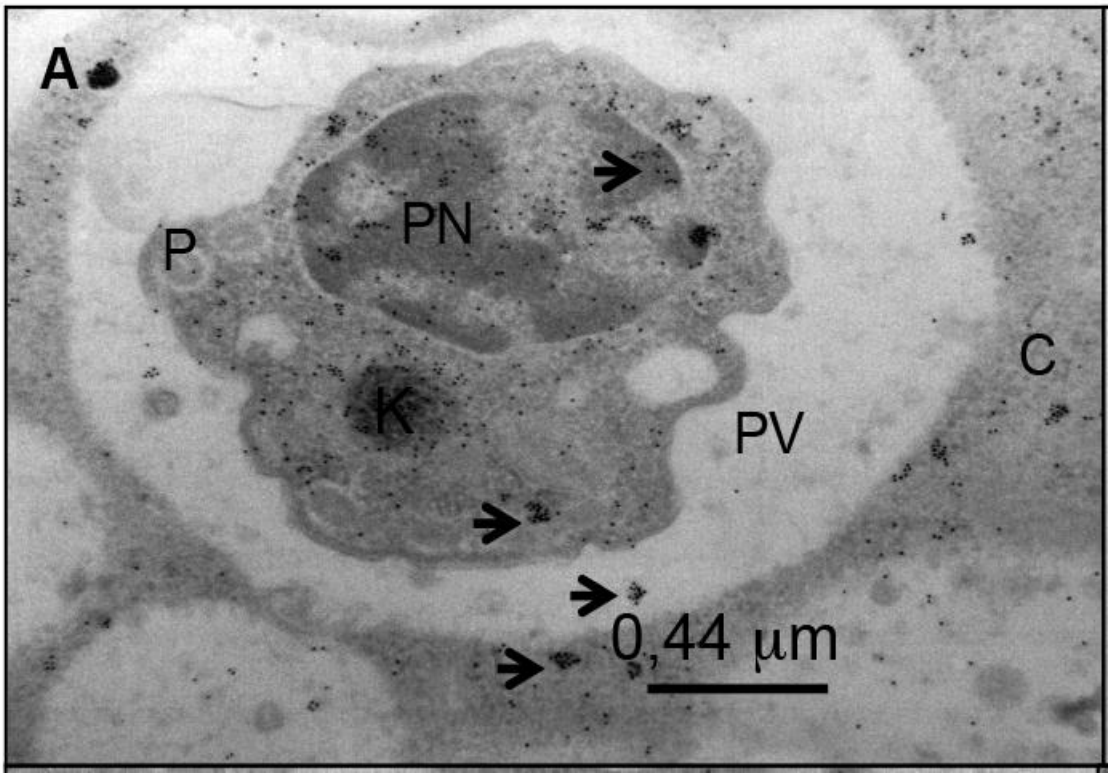

Figure 14: Vesicle-like Structures with Positive Gold Label were Observed at 2h Post-Infection.

Electron microphotograph amplification of a host cell 2h PI. A parasite (P) is inside a parasitophorous vacuole (PV) with gold particles detected in the parasite nucleus (PN), Kinetoplast (K) and on vesicle-like structures (arrows), which can also be observed in the host cell cytoplasm (C).

- **Calreticulin Concentration is Higher in Infected Cells**

As cross-reactivity was still an issue in the studies performed with the anti-TcCRT PoAb, the number of gold particles/µm^2, in different compartments of the host cell, was quantified as described in the Methods Section. Non-infected cells showed lower number of gold particles in the analyzed cellular compartments, compared to 2h PI ($p<0.05$ in cytoplasm, $p< 0.01$ in nucleus, Fig.15A). A similar situation was observed when compared to 4h PI ($p< 0.01$ in nucleus and cytoplasm, Fig.15B). The only variation between the two conditions was the label in the cytoplasm, which increases at 4h PI. When non-infected cells were compared to 6h PI, the nucleus was the only compartment that presented more gold particles in the infected cells (Fig.15C). In the parasitophorous vacuole, the number of gold particles decreases at 6, compared to 2 and 4h PI.

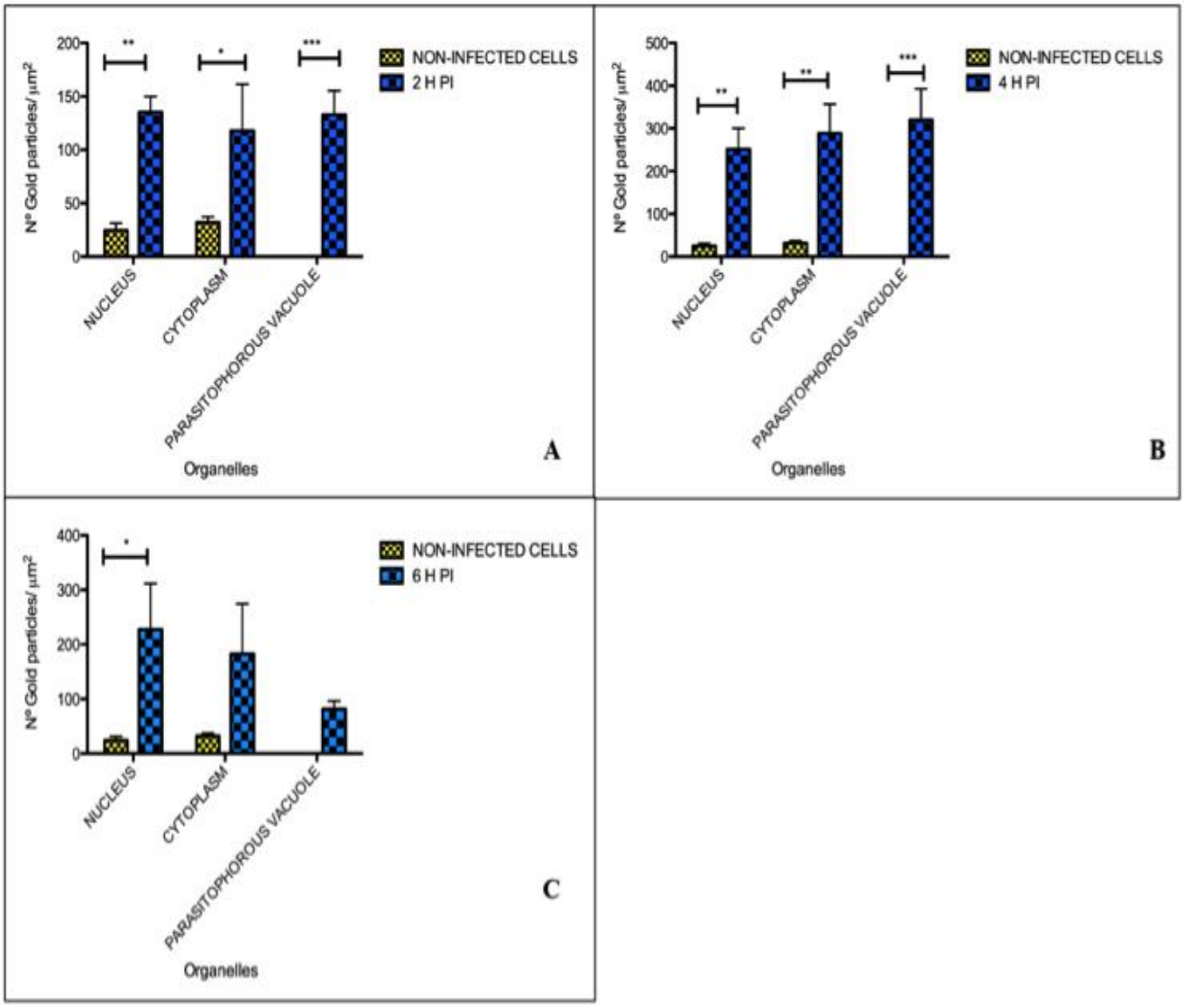

Figure 15: Number of CRT Molecules Detected with the Polyclonal Anti-rTcCRT Antibody is Higher in Infected Cells

At 2 and 4h PI, more gold particles are detected in the nucleus and cytoplasm (**A** and **B**) when compared to non-infected cells. At 6h PI (**C**) a larger number of gold particles is detected only in the nucleus, as compared to the non-infected counterpart. The average number of particles found in the parasitophorous vacuole is included for comparison purpose.

A-C: Two-way ANOVA * = p< 0.05 **= p< 0.01 ***= p< 0.001. Bars: Standard deviations.

- **TcCRT is Detected with a Monoclonal Antibody in Free Parasites**

The second validated detector probe for immunocytochemistry was the monoclonal anti-TcCRT E2G7, which in two different experiments, showed no cross-reactivity with RAW 264.7 WCE (see Figs.8 and 9).

With this detector probe, in free trypomastigotes (Fig.16A), gold particles are observed almost exclusively in the kinetoplast. In non-infected RAW 264.7 murine macrophages (Fig.16B), some gold particles are detected in the nuclear heterochromatin, and also in the cytoplasm, most likely as a non-specific background label. In free epimastigotes (Fig.16C) label is observed basically in the nucleus. Few molecules are detected in the kinetoplast.

On infected cells, at 2h PI (Fig.17A), gold particles were observed in the parasitophorous vacuole, and in the host cell. Again, in the parasite, the particles were detected almost exclusively in the kinetoplast. In the host cell, some gold particles were observed in nuclear heterochromatin.

At 4h PI (Fig.17B), gold particles were observed in the parasitophorous vacuole. As previously detected (Fig.16A, 17A), there is a high-density label in the kinetoplast. However, at this point some gold particles are detected on the parasite nucleus and cytoplasm. In the host cell, some particles are observed in nucleus and a few in the cytoplasm.

At 6h PI (Fig.17C), two parasites were observed inside parasitophorous vacuoles. In both cases, a high gold particle concentration is detected in their kinetoplasts. Much lower gold particle concentration is detected in the parasite nucleus and cytoplasm. No gold particles were observed in a 6h PI sample incubated with an anti-HuCD45 mouse IgG1 (isotype negative control, Fig.17D), or in a free trypomastigotes sample incubated with just the secondary antibody (Fig. 17E).

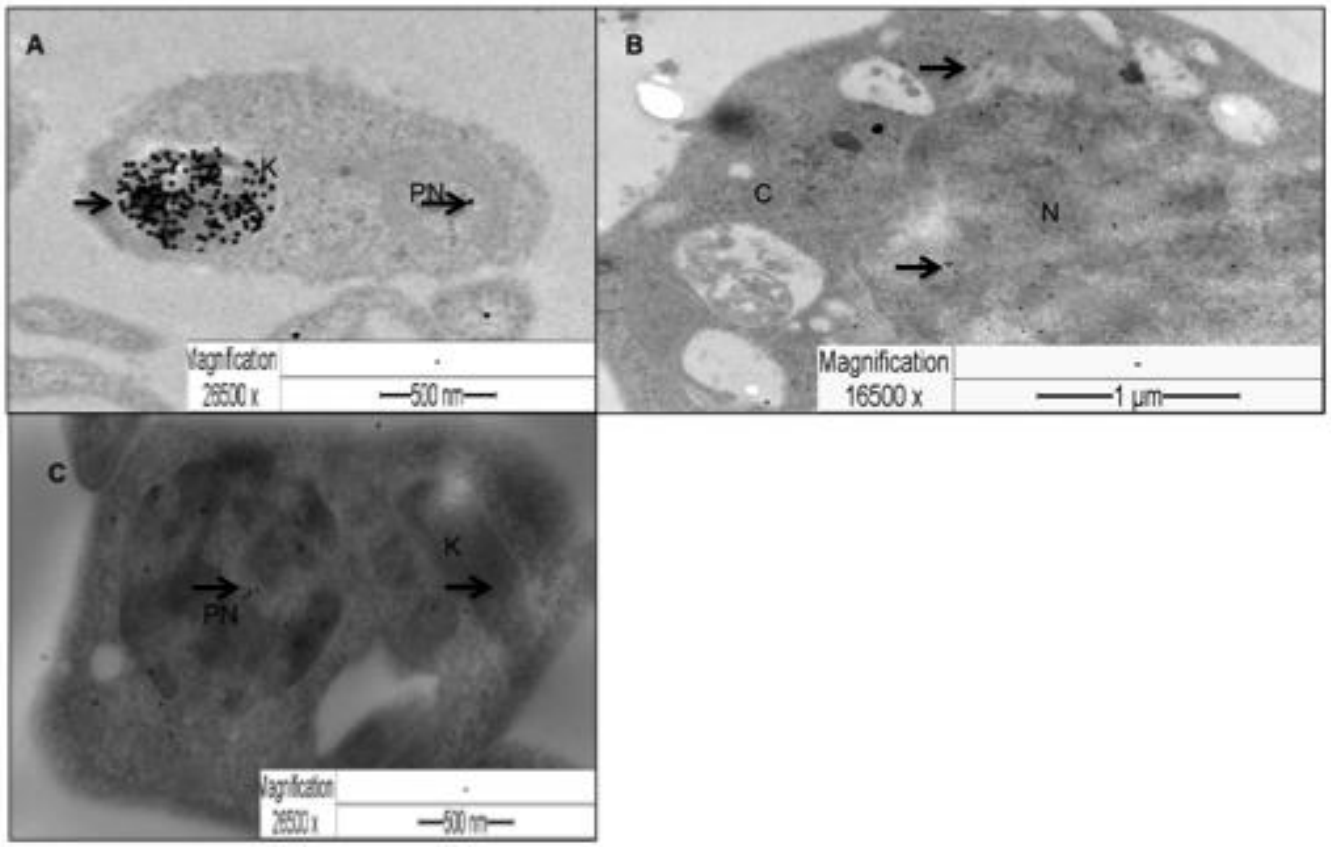

Figure 16: MoAb E2G7 Anti-TcCRT detects TcCRT in Free Parasites

Electron microphotographs of non-infected cells and free parasites are shown. Gold particles are observed in: **A.** A free trypomastigote, mainly in an oblique section of the kinetoplast (K); **B.** A non-infected murine macrophage, mainly in nucleus as a background label; **C.** A free epimastigote, mainly in the nucleus. A longitudinal section of an almost empty kinetoplast section is also presented.

In host cell: N: Nucleus, C: Cytoplasm. In parasites: PN: Parasite nucleus, K: Kinetoplast. All samples were incubated with E2G7 anti-TcCRT monoclonal antibody, 0.00489 µg/µl, followed by the corresponding gold-labeled secondary antibody, 1/20 v/v. Arrows: Positive signals.

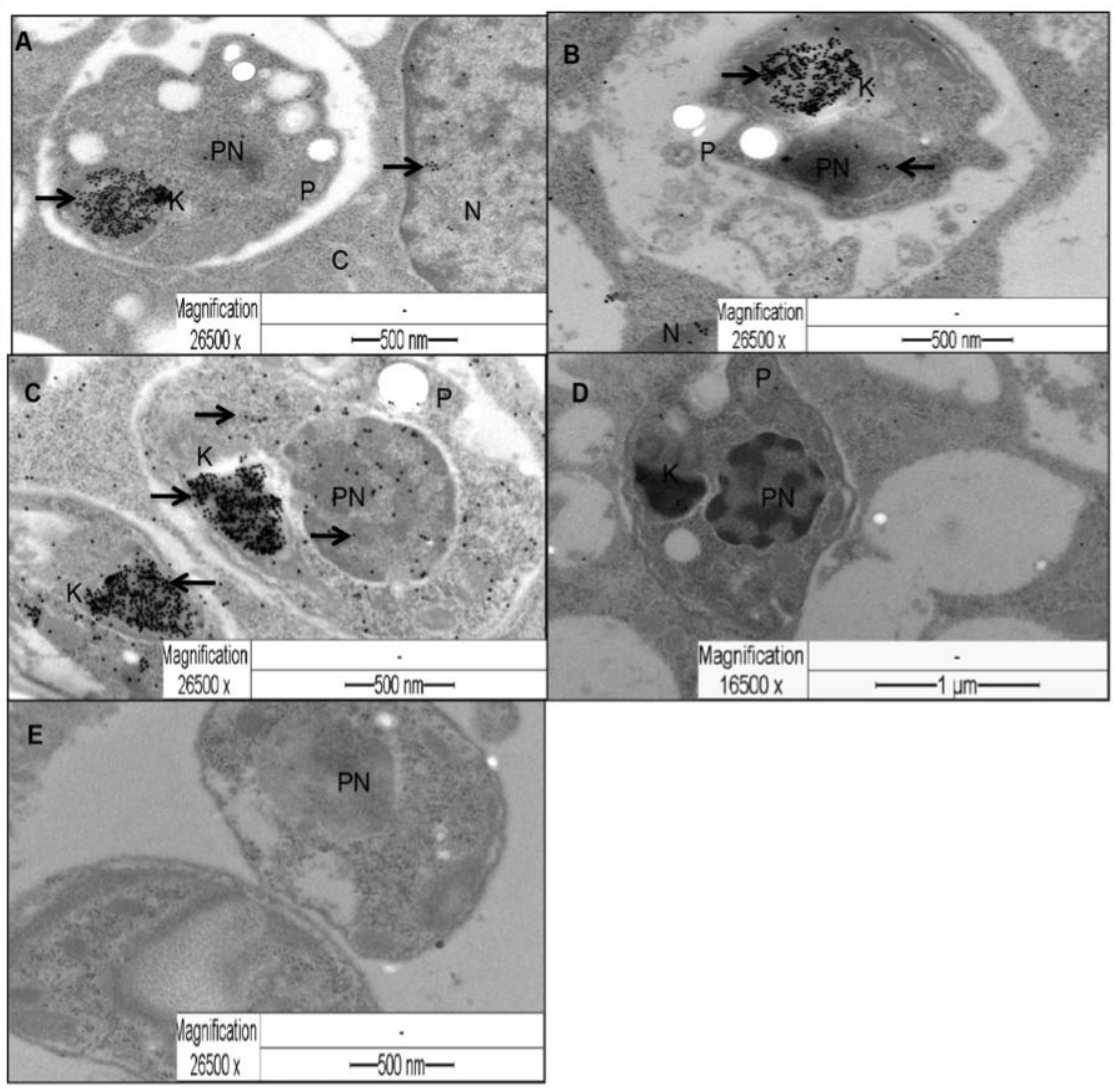

Figure 17: TcCRT is Mainly Found in the Parasite Kinetoplast in Infected Cells

Electron microphotographs of infected cells are shown. Gold particles are observed at **A.** 2h PI, mainly in the parasite kinetoplast; **B.** 4h PI, mainly in the parasite kinetoplast, fewer in the parasite nucleus; **C.** 6h PI, in two intravacuolar parasites, mainly in the kinetoplast, but also in the parasite nucleus and cytoplasm. In negative control samples **D.** 6h PI and **E.** Free trypomastigotes, no gold particles were observed.

In host cell: N: Nucleus, C: Cytoplasm. In parasites: P: Parasite, PN: Parasite nucleus, K: Kinetoplast.

Samples were incubated with: **A-C:** E2G7 anti-TcCRT monoclonal antibody, 0.00489 µg/µl; **D:** Anti-HuCD45, mouse IgG1 0.005 µg/µl, isotype negative control; **E:** Anti-mouse IgG conjugated to colloidal gold (18 nm), 1/20 v/v. Arrows: Positive signals.

- **TcCRT Presence is Higher in the Parasite Kinetoplast of Infected Cells, as compared to Free Trypomastigotes or Epimastigotes**

The improvement in sensitivity, and the use of a larger gold particle size and the monoclonal antibody, allowed a simple naked-eye visual quantification of the minimum number of molecules detected in different stadia of the parasite. A representative set of results corresponding to free and non-free parasites is shown in Figure 18. A major number of TcCRT molecules are detected in trypomastigote kinetoplast when the parasite is *inside* the host cell (Figs.18A, 18D) compared to free trypomastigotes (Fig.18B) or free epimastigotes (Fig.18C), which indicates a cumulative presence in this organelle in infective trypomastigotes.

3.- Evaluation of variations in surface MHC-I molecules on infected murine macrophages (Hypothesis II).

3.1 Flow Cytometry

- **MHC-I Positive Cells Decrease Post Infection**

CRT is key on the MHC-I folding process, as it is part of the peptide loading complex [11]. An increase of CRT molecules was detected with the polyclonal anti-TcCRT antibodies in infected host cell cytoplasm (Fig.15). Therefore, we asked whether this CRT expression correlates with that of MHC-I molecules. By flow cytometry, surface MHC-I positive cells were identified as described in the Methods Section, in non-infected and infected RAW 264.7 cells. Less MHC-I positive cells are detected at 2 and 4h PI as compared to non-infected cells, while the 6h PI sample is similar to the non-infected counterpart (Figs.19A, 19C), which suggests a high cell mortality at early times post-infection. The percentage of maximum fluorescence, which is indicative of surface expression of MHC-I molecules per cell, was similar in all samples studied, which is indicative of no variation of the expression of MHC-I molecules in the murine macrophage (Fig.19B).

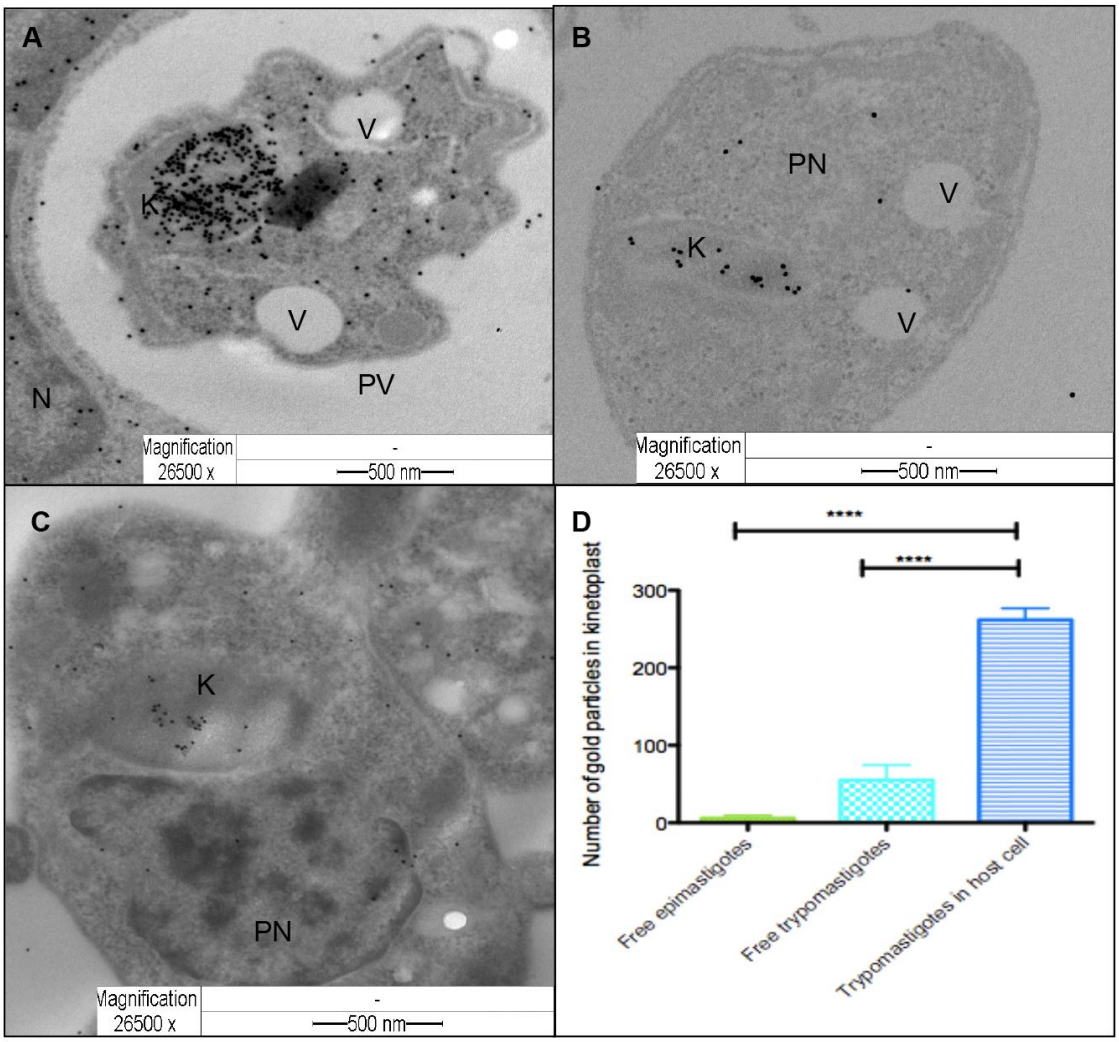

Figure 18: The Number of TcCRT Molecules is Higher in the Parasite Kinetoplast of Infected Cells, as compared to Free Trypomastigotes or Epimastigotes

Electron microphotographs of infecting and free parasites are shown. Gold particles are detected in **A.** A 6h PI sample, mainly in the trypomastigote kinetoplast (K), but also detected in the parasite nucleus and host cell cytoplasm. **B.** A free trypomastigote, almost exclusively in the kinetoplast (K). **C.** A free epimastigote, in nucleus and kinetoplast. **D.** The number of gold particles detected in kinetoplast sections, is higher in infecting parasites (n =6 for free trypomastigotes and epimastigotes, n= 5 for trypomastigotes in the host cell).

A-C: MoAb E2G7 anti-TcCRT 0.00489 μg/μl; **D:** One-way ANOVA analysis, **** = $p < 0.0001$. In host cell: N: Nucleus. In parasites: PV: Parasitophorous vacuole, PN: Parasite nucleus, V: Vacuoles, K: Kinetoplast.

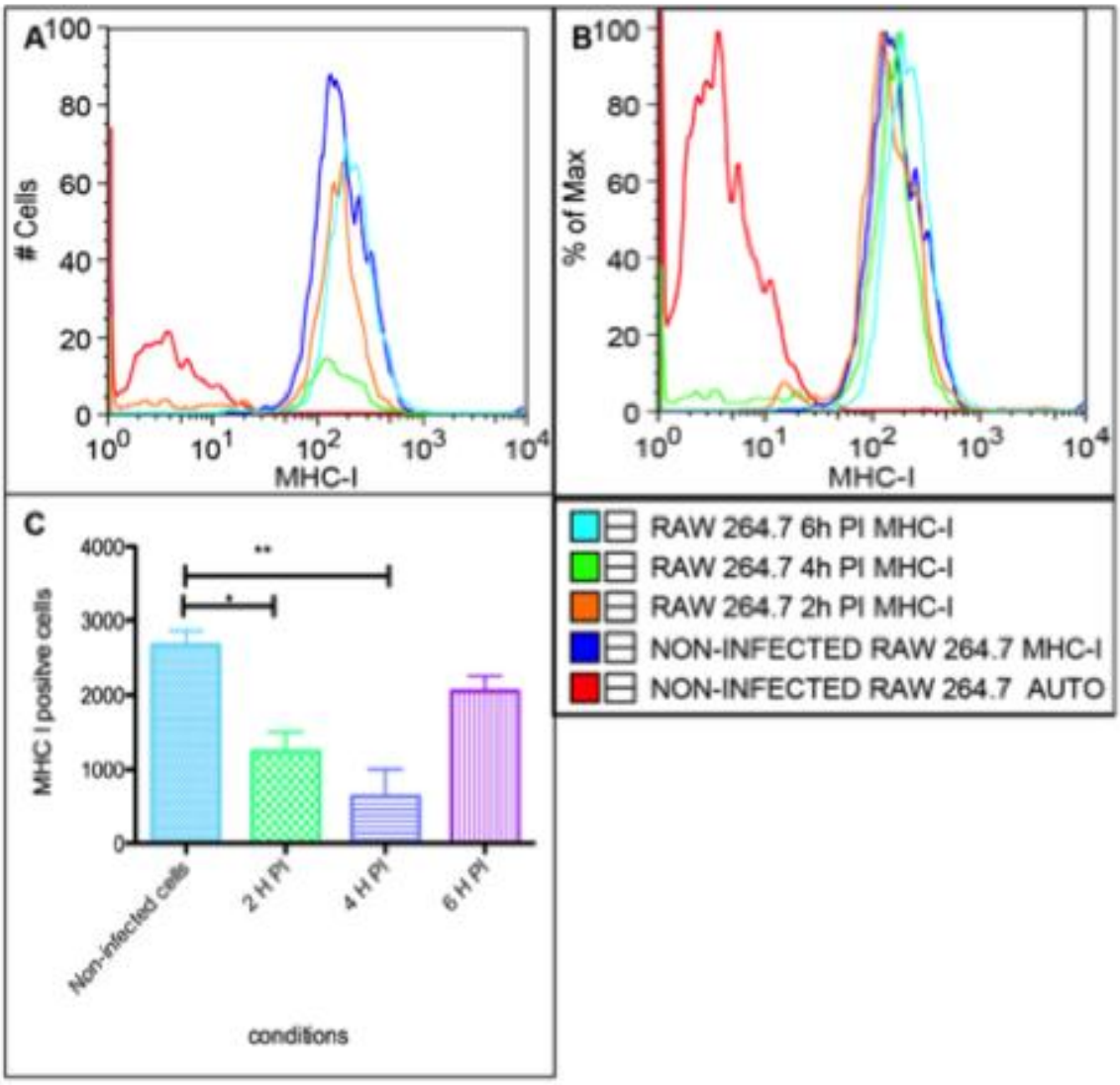

Figure 19: MHC-I Positive Cells Decrease at 2 and 4, but not at 6 h PI, as Detected by Flow Cytometry

Representative cytometry histograms are shown. **A:** The number of MHC-I positive cells decreases at 2 and 4h PI, while the 6h PI sample remained similar to the non-infected counterpart; **B:** The percentage of maximum fluorescence was similar in all samples analyzed, which is indicative of no variation of surface MHC-I molecules per cell; **C:** Statistical analysis of MHC-I positive cells. One-way ANOVA analysis of data, * = $p< 0.05$, ** = $p< 0.01$. Bars = Standard deviations.

DISCUSSION

TcCRT is currently accepted as a virulence factor, due to its relevance in the infectivity process, inhibition of the classical and lectin pathways of the complement system and inhibition of angiogenesis and tumor growth [14, 15, 17-20].

Although in its amino acid sequence it possesses an ER-retrieval signal, KEDL, on its carboxy-terminus domain, its intracellular localization inside the parasite is diverse. Previous reports showed the presence of TcCRT in the ER, as expected, but also in the Golgi, cytostome, on vesicles near the flagellum pocket, on the cytosol, and on the nucleus and kinetoplast, on *free* trypomastigotes and epimastigotes. This evidence suggests a possible secretion pathway for TcCRT [53]. It should be pointed out, however, that in this publication results using a pre-immune serum, as negative control, are not shown. For this reason, the magnitude of cross reactivity of the polyclonal antiserum used with other parasite molecules cannot be correctly assessed.

More recently, this evidence is supported by other studies where two populations of vesicles, secreted by the *free* parasite to the extracellular milieu, were analyzed and their protein cargo characterized. TcCRT is among the 367 proteins identified [54]. The analyses of the vesicle cargo and localization of TcCRT were performed in both free trypomastigotes and epimastigotes [53, 54]. There is no evidence in the literature, with regard to TcCRT localization when the parasite is located inside the host cell. We have addressed this important issue in this Doctoral Thesis.

In order to study the TcCRT localization once the parasite is *inside* the host cell, it was first necessary to evaluate and standardize possible antibodies to be employed as detector probes in several immunocytochemistry procedures.

Different experiments were performed in order to validate the specificity of the three antibodies as summarized in Figures 6, 7, 8 and 9, and also in Figure 22, this one shown I ANNEX I

When the anti-TcCRT PoAb was tested, there was a cross-reactive detection of a 58 kDa band when a RAW 264.7 WCE was employed as antigen

source (Fig.6). Considering that CRT is highly conserved among species [10] and that the polyclonal serum employed has a titer of 10^{-6} the present results were expected. As dilution increases, the cross-reactivity minimizes, which makes this antibody a suitable candidate to be employed as detector probe in immunocytochemistry. The former result was corroborated as with a homologous anti-MmCRT PoAb a tenuous band of 58 kDa is detected (Fig.7).

An anti-TcS PoAb detected an immunoreactive band of 46 kDa in at lest 3 cell lines. Attempts to validate this antigenically recognized putative MmCRT, as conventional murine CRT, implied a variety of experimental approaches that rather escape from the main goals of this thesis. For this reason this subject is presented as an ANNEX I, in this document. Given the results obtained, this anti TcS PoAb is not a viable option to be employed as a detector probe in the immunocytochemical procedures described herein.

Since the anti-TcCRT PoAb still had serious limitations to be employed as detector probe in immunocytochemistry (cross-reactivity, though minimized, was still a problem), an E2G7 anti-TcCRT MoAb was also validated. Its specificity was confirmed as it recognized rTcCRT and eTcCRT from different sources (purified and direct from an epimastigote extract) (Fig.8A). No band was detected in a RAW 264.7 WCE, which suggest this antibody would be appropriate as detector probe of the parasite molecule in immunocytochemistry.

The purification process of eTcCRT did not involve stringent methods, which would explain, in part, why it was necessary 300 ng of total protein compared to the 10 ng of rTcCRT. When both extracts, RAW 264.7 and epimastigote, were pre-incubated with rTcCRT, there was predominant detection of the recombinant molecule, as expected (Fig.8B). However, we cannot rule out that in the epimastigote extract eTcCRT was also detected, but the signal was “masked” by the detection of rTcCRT.

The former validation process was performed by IWB, not a physiological condition, as the proteins in the extract are subjected to heat denaturation and reduction, among other stringent manipulations. Thus, the epitopes recognized in the murine extract would not include the conformational epitopes that would be

recognized by the polyclonal serum as the recombinant protein used for the rabbit immunization was in a physiological state.

As a more physiological approach, through an indirect ELISA, the E2G7 MoAb was also tested. The rTcCRT molecule is specifically captured by solid-phase bound E2G7 MoAb, when compared to several controls (Fig. 9A). However, when the parasite and host cell extracts were employed as CRT source, there was no capture of endogenous CRT. Only when the extracts were pre-incubated with rTcCRT a positive signal was observed (Fig. 9B). This result can be explained, in part, as given the chaperone capacity of CRT, in the extract context, the endogenous molecule binds to several other proteins present in the extract, through the epitope recognized by the E2G7 MoAb. Thus, no capture is possible. Alternatively and/or concomitantly, the relative quantity of TcCRT in the epimastigote extract did not reach the minimum necessary to be captured by the monoclonal antibody.

In synthesis, the present results allowed to validate two antibodies as detector probes for immunocytochemistry, a polyclonal serum anti-TcCRT and a monoclonal antibody E2G7.

As the different fixation conditions required for immunocytochemistry do not allow a proper fixation of lipids and preservation of structures, Figure 10 shows a topographic control of each condition, in which organelles are distinguished. In non-infected RAW 264.7 cells, we observed ribosomes (Fig.10A). Mammalian ribosomes are about 30 nm diameter, serving as indicators of resolution. Thus, 10 and 18 nm gold particles, being more electron-dense than ribosomes, should be adequately resolved. Properly resolved organelles were observed at 2 h PI, with the parasite inside a parasitophorous vacuole (Fig.10B). Interestingly, at 4h PI (Fig.10C), the host cell is extensively vacuolated. This might be due to the infection process at this time gate. At 6h PI, a minimum of three parasites was observed free in the host cell cytoplasm (Fig.10D). In this case, due to the time post-infection, they are probably three different parasites that infected this host-cell.

In order to validate the technique, non-infected RAW 264.7 cells were

incubated with the respective anti-MmCRT serum. Gold particles are observed mainly in nucleus and fewer molecules were observed in cytoplasm (Fig.11). Interestingly, no gold particles were observed in ER. This could be due to several factors, such as a low concentration of specific anti-MmCRT antibodies. Using the recommended dilution for this antibody, detection was marginal in IWB and in immunocytochemistry. However, this procedure resolved gold particles, an indication that the technique provides the proper resolution to track TcCRT once the parasite is inside the host cell.

Using a polyclonal anti-rTcCRT serum, we observed more gold particles in infected cells (Fig.15). However, as expected with polyclonal antibodies, some cross-reactive background is also present in non-infected cells (Fig.12A) (In order to compare the electron density of gold particles and ribosomes, Figs.10A and 12A should be considered together). Considering that CRT is highly conserved among species, it is likely that a rabbit antiserum, generated against the parasite molecule, will recognize the host-cell molecule, in those epitopes common to TcCRT and MmCRT. Through the titration process, this cross-reactivity was minimized.

In free epimastigotes (Fig.12B), TcCRT was observed mainly in the nucleus, as previously described [53]. On the other hand, in free trypomastigotes (Fig.12C), gold-particles were detected on the flagellum emergence zone and kinetoplast. This result is interesting, in particular the high label concentration in the kinetoplast, concordant with previous results [53].

TcCRT is externalized from the ER to the flagellum emergence zone, where it co-localizes with C1q, so the concentration in this particular compartment is in agreement with previous results obtained in confocal fluorescence microscopy [15].

Some particles were observed in vesicle-like structures. As previously reported, TcCRT is part of the protein cargo in vesicles secreted by the parasite [54], but it was not detected *in situ inside* the vesicles, but *outside* the trypomastigote. This observation may complement the previous work, supporting a secretory pathway for TcCRT [53]. It cannot be ruled out the possibility that, since

these parasites were harvested from the supernatant of infected VERO cells, the circular vesicle-type structure outside the parasite, where CRT was detected, may derive from the VERO host cell. However, its attachment to the parasite plasma membrane supports its parasite origin. At 4h PI, other circular structures, with positive gold label, were observed in close proximity to the parasitophorous vacuole outside the host cell (Fig.20A), which can be compared to the vesicle-like structures in free trypomastigotes (Fig.20B). The vesicle-like structures seen in Figures 12C and 20A are 35-38 nm in diameter (data not shown), consistent with those previously described for metacyclic trypomastigotes [54]. Even though is not possible to determine, on the infected cell, the origin of the putative microvesicles, its localization could suggest its parasitic origin, although it cannot be discarded its host cell origin.

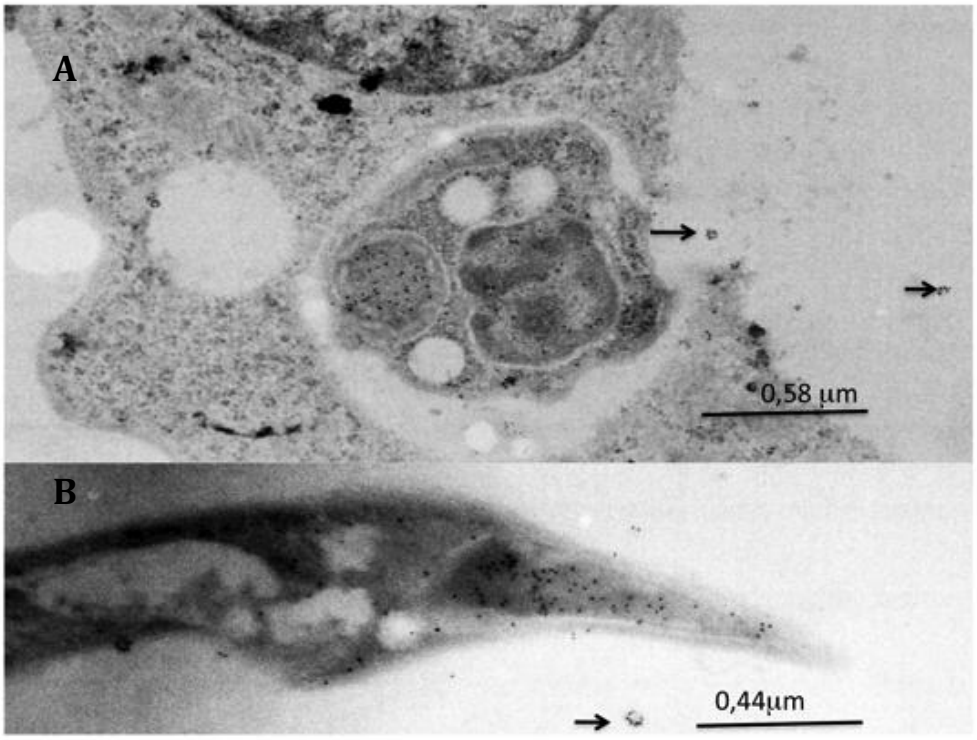

Figure 20: Vesicle-like Structures with Positive Label were Observed in Free Trypomastigotes and Infected Cells.

Electron microphotographs (30,000x) of: **A.** 4h PI cell; **B.** Trypomastigote, where vesicle-like structures with positive gold label were observed. All samples were incubated with anti-rTcCRT polyclonal serum 1/32,000 v/v followed by gold-

labelled secondary antibody 1/20 v/v. Note: Figure 20B was shown previously as part of Fig.12. This time is only shown to stress the possibility of microvesicles existence.

A critical condition to determine whether if the structures observed with positive gold label are microvesicles, is the presence of a membrane, which in all structures observed, could not be appreciated at this resolution as fixation conditions for immunocytochemistry do not allow proper fixation of membranes, and also for the electron-dense gold particles present. Thus, is still speculative whether these circular structures are effectively microvesicles. Further work is necessary in this area but, given the time constraint, outside the context of this thesis.

On infected cells, (Fig.13) gold particles were observed in different organelles in the parasite and in the host cell. Interestingly, the DNA containing organelles, kinetoplast and the parasite nucleus, were those where a high-density label was observed, concordant with previous reports in the literature [53]. At 2 (Fig.13A, 14) and 6h PI (Fig.13C), when the parasite is observed inside the parasitophorous vacuole, similar vesicle-like structures are detected with positive gold label inside the parasite, in the parasitophorous vacuole, and its surroundings, in the host cell cytoplasm. These structures were observed previously inside metacyclic trypomastigotes and described as vesicles [53]. All the results mentioned above supports a secretory pathway for TcCRT.

In the host cell, some particles are observed in the cytoplasm and nucleus. Due to the sensitivity of the technique used, it is not possible to discriminate, at this point, the origin, parasite or host cell, of the protein that is detected by the anti-rTcCRT polyclonal serum. In favor of the possibility that the recognized protein is indeed CRT, from parasite or host cell origin, is the fact that the antiserum was raised against the pure recombinant parasite protein. Given the evolutionary distance between trypanosomatids, on the one hand, and mammal (rabbits and mice), on the other, most of the epitopes that are finally immunogenic in the rabbit

are probably of trypanosomatid origin. Rabbit antibodies generated against those few epitopes shared by murine and *T. cruzi* CRT should be undetectable in properly diluted sera, a simple strategy tested in our experiments.

At 4h PI (Fig.13B), a parasite is observed outside the host cell, probably before been phagocytosed. Similar to previous results, in the parasite, high-density label was observed in nucleus and kinetoplast. In the host cell, gold particles were observed in nuclear heterochromatin and cytoplasm, consistent with the previous results. No extensive vacuolization could be observed in the host-cell, a phenomenon perhaps only present when the parasite is *inside* the host cell, at this time gate. None of the controls performed in a 6h PI sample, in the absence of primary antibody (Fig.13D) or with pre-immune serum (Fig.13E), showed gold particles, an indication of specific labelling.

Despite the cross-reactivity of the polyclonal anti-rTcCRT serum, there are more gold particles/μm^2 in nucleus and cytoplasm from infected cells, as compared to the non-infected counterpart (Fig.15). Thus, at 2h PI, there are more CRT molecules in nucleus and cytoplasm (Fig.15A), reaching a maximum at 4h PI (Fig.15B), in all cellular compartments analyzed.

Possible explanations for these results include: **i)**. TcCRT is secreted by the parasite, and at 4h PI is accessing the host cell cytoplasm, and the nucleus. Perhaps TcCRT accesses the host cell cytoplasm (*i.e:* via vesicles), with unsuspected consequences in immune evasion strategies. Controversial evidence can be found in the literature, where infection with *T. cruzi* modulates negatively the over-expression of MHC-I on the membrane of the host cell, when induced with LPS, an extremely potent and pleiotropic PAMP (Pathogen associated molecular pattern) [64] and other studies showed no effect on MHC-I at all [65]; **ii)** Alternatively or concomitantly, a MmCRT peak was observed at 4h PI, possibly overexpressed during infection, is detected by anti-rTcCRT antibodies present in the polyclonal serum, that cross-react with MmCRT.

At 6h PI, there are more CRT molecules compared to the non-infected counterpart only in the nucleus (Fig.15C). In cytoplasm, no significant differences were obtained. In the parasitophorous vacuole, at 6h PI, there is a decrease in

the number of gold particles detected, compared to 2 or 4h PI, which could be an indication of TcCRT mobilization at this level.

The E2G7 MoAb is the other detector probe which was validated to be used in this immunocytochemical study, since it does not detect murine proteins in IWB or indirect ELISA when a RAW 264.7 WCE was employed as antigen source (see Results section, 1.1 and 1.2).

In free trypomastigotes (Fig.16A), gold particles are detected almost exclusively in the kinetoplast and very seldom in other organelles. Whether the epitope recognized by the monoclonal antibody is exposed correctly mainly in the kinetoplast, remains to be determined. Previous results [53], and those obtained with our polyclonal anti-rTcCRT antibody, where TcCRT can be observed mainly in the kinetoplast, are basically concordant to those obtained with the E2G7 MoAb. In non-infected RAW cells (Fig.16B), some particles are detected by the E2G7 MoAb in the nucleus and cytoplasm as a natural background label.

On free epimastigotes (Fig.16C) label is observed mainly in nucleus, and few particles are detected on kinetoplast, which is consistent with previous results [53]. However, label is not as dense as it is on trypomastigote kinetoplast, which suggests differences related with the parasite stage. Perhaps, since TcCRT is a key virulence factor, trypomastigotes synthesize more molecules than epimastigotes do, since the latter is a non-infective form. In fact, recent results from our laboratory indicate that TcCRT is present in both epimastigotes and trypomastigotes, but only the latter are able to translocate the molecule from the ER to the exterior [15].

On infected-cells (Fig.17) the common pattern is a significant label on the kinetoplast, in all conditions analyzed (2, 4 and 6h PI). Only a few molecules can be observed in the parasite nucleus and in the host cell cytoplasm and nucleus.

Interestingly, the E2G7 MoAb apparently discriminates TcCRT according to its functional state. For example, while it does not recognize externalized endogenous TcCRT in flow cytometry, most likely because the epitope is not accessible to the antibody (Ferreira *et al*, unpublished), it does recognize the molecule in different

compartments of the free and infecting parasites.

Remarkably, the kinetoplast is the organelle where gold particles are detected in a high concentration using both, the monoclonal anti-TcCRT antibody and the polyclonal anti-rTcCRT serum in all samples analyzed. According to previous reports, using polyclonal anti-TcCRT antibodies, the kinetoplast is the organelle that presents more gold particles/μm^2 in free trypomastigotes [53].

Since different sections of the parasite kinetoplast were analyzed, depending on the relative direction of the cut (oblique, transverse or longitudinal) and its position in the organelle, different views can be obtained in TEM. Due to statistical possibilities, oblique and sagittal sections were observed more often. These possible cuts and the views obtained are summarized in Figure 21 (assuming that the kinetoplast has an overall cylindrical shape).

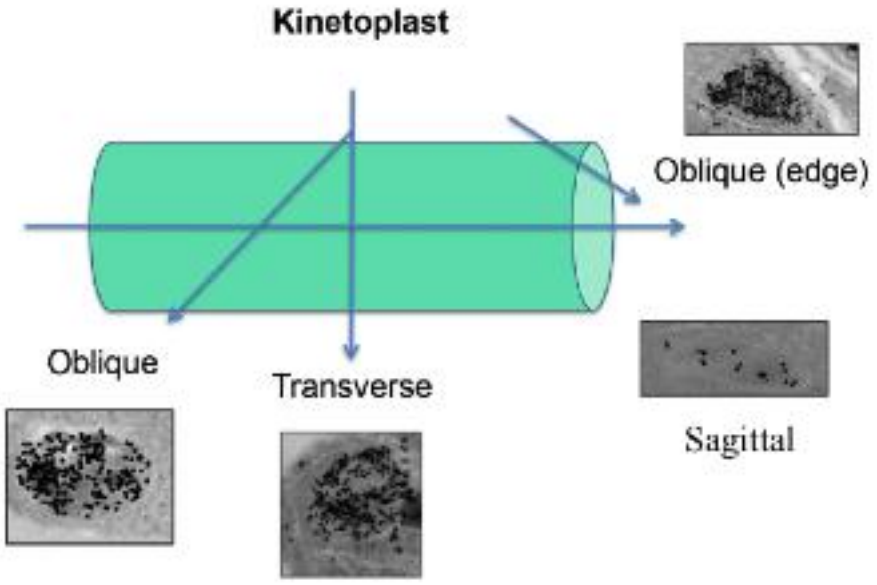

Figure 21: TcCRT Detection in Different Kinetoplast Sections with E2G7 MoAb.

TcCRT was detected in different kinetoplast sections. Schematic representation of the kinetoplast and possible cut sites are shown. Most of the sections observed were transverse or oblique. Only a few sections were sagittal (kinetoplast dimension is 1 μm in length, 0.1 μm in depth, and the sections were 700 Aº thick).

The kinetoplast, as an organelle, is near the flagellum emergence zone (Fig.12C) [66], where condensation of vesicles has been reported [55]. Perhaps, one possible explanation of the high-density label in the kinetoplast is to act as a reservoir of TcCRT before it can access the flagellum pocket zone during the externalization process.

Other possible role is gene expression/transcription regulation [67]. Mammal CRT binds to nuclear glucocorticoid receptors, regulating its activity [40, 42], which is key in cell signaling transduction that leads to gene expression/repression. Considering that the kinetoplast, as mammalian mitochondria, has DNA, this still speculative possibility cannot be completely ruled out. Kinetoplast DNA (kDNA), however, is quite unique and different in its organization and transcription mechanism. It consists of two molecular species, minicircles and maxicircles, which form a single giant network of DNA localized adjacent to the basal body. kDNA minicircles are heterogeneous and usually there is more than one class of minicircle in the same cell. However, they share a strongly conserved region, which represents approximately 10% of the minicircle length. kDNA maxicircles, on the contrary, are more conserved, and actively transcribed. Little is known about the regulation mechanism of transcription in both, mini and maxicircles [68, 69].

A third possibility rises since CRT, in general, regulates Ca^{+2} storage and signaling [33, 67, 70]. A proper Ca^{+2} influx between the ER and mitochondria is key for mitochondrial function. Moreover, when a truncated form of CRT is expressed in cells, an altered Ca^{+2} response is obtained in ER and mitochondria [70]. If the kinetoplast plays a central role in the mitochondrion, it might require a proper Ca^{+2} influx between this organelle and the ER, thus providing an additional functional explanation for the unusual large concentration of TcCRT in this organelle.

In synthesis, at this point we can not discriminate whether the kinetoplast is a simple stopover or storage reservoir for TcCRT, before its externalization, or alternatively or concomitantly, that the parasite molecule plays a role in gene transcription regulation and/or Ca^{+2} storage and signaling in this organelle.

The specificity of the anti-TcCRT E2G7 MoAb is warranted since an anti-

HuCD45 monoclonal antibody (mouse IgG1, isotype control, Fig.17D), and the secondary antibody only (Fig.17E), did not mediate the detection of gold particles in relevant antigenic preparations, as detected in TEM.

Conversely, in infecting trypomastigotes, there were a higher number of TcCRT molecules than in free trypomastigotes or epimastigotes in kinetoplast sections (Fig.18). This result is concordant with former results obtained by reverse-transcription PCR. In this assay, TcCRT mRNA increases in the first 24h post-infection, although from different cells, obtained after larger times post-infection [17].

Since CRT is a key molecule in the MHC-I folding process, as it is part of the peptide loading complex, infection might influence the surface expression of MHC-I molecules on infected cells. Less MHC-I positive cells were detected at 2 and 4h PI, while the 6 h PI sample remained similar to the non-infected counterpart (Fig.19A, 19C). When the percentage of maximum fluorescence was analyzed, in order to evaluate MHC-I surface molecules per cell, no differences between experimental time gates were found, which indicates that MHC-I surface molecules per cell remained similar in all samples analyzed (Fig.19B).

Possible explanations to the former results include: **i).** Since the number of MHC-I positive cells on the gate, decreased substantially in the infected cells, at 2 and 4h PI, the possibility exists that the infective challenge killed a proportion of these cells. Furthermore, extensive vacuolization is observed at 4h PI. This, together with the fact that CRT is externalized in apoptotic cells, as a damage-associated molecular pattern (DAMP), thus promoting clearance of the apoptotic cells [71-73]; **ii).** Alternatively or concomitantly, TcCRT accesses to the host cell cytoplasm at 2h PI, reaching its peak at 4h PI. Whether TcCRT accesses to host cell ER and there competes with MmCRT in promoting the correct MHC-I molecule folding is unknown. In agreement with this possibility, the peak of CRT detection is at 4h PI, the same time gate when less MHC-I positive cells are detected. Moreover, the vesicle-like structures observed with the anti-rTcCRT polyclonal serum (Figs.12C, 13A, 19A) supports the access of TcCRT into the host cell cytoplasm.

Perhaps, the parasite uses its CRT not only to access the host cell [17], but also to evade antigen presentation through secretion into the host cell cytoplasm. However, its secretion may induce translocation of the host cell CRT, which can be recognized as a DAMP by innate immune mechanisms, with subsequent elimination of the infected cell during the first hours post-infection.

Finally, based on the results presented here, in Fig. 22, possible pathways that TcCRT could follow from the parasite ER to the parasite exterior are presented. Is important to stress that this proposal is for a parasite located *inside* the host cell. A recognized view is that a peptide signal allows TcCRT to exit the parasite ER, followed by access to the parasite Golgi where it suffers post-translational modifications previous to its externalization. Once modified in the Golgi apparatus, it converges in the parasite kinetoplast (where it might have roles in transcriptional regulation of the kinetoplast DNA, or Ca^{+2} signaling regulation, or simply accumulates there for subsequent exteriorization). Outside the parasite, TcCRT may cross the parasitophorous vacuole and access the host cell cytoplasm (alternatively and not represented in the Figure, TcCRT may access the host cell cytoplasm once the parasite exits the parasitophorous vacuole). The speculation continues assuming that, there, through mechanisms similar to those used by virus or bacterial toxins, TcCRT could access the host cell ER. Over there, competition with the host cell CRT for MHC-I molecules could be established.

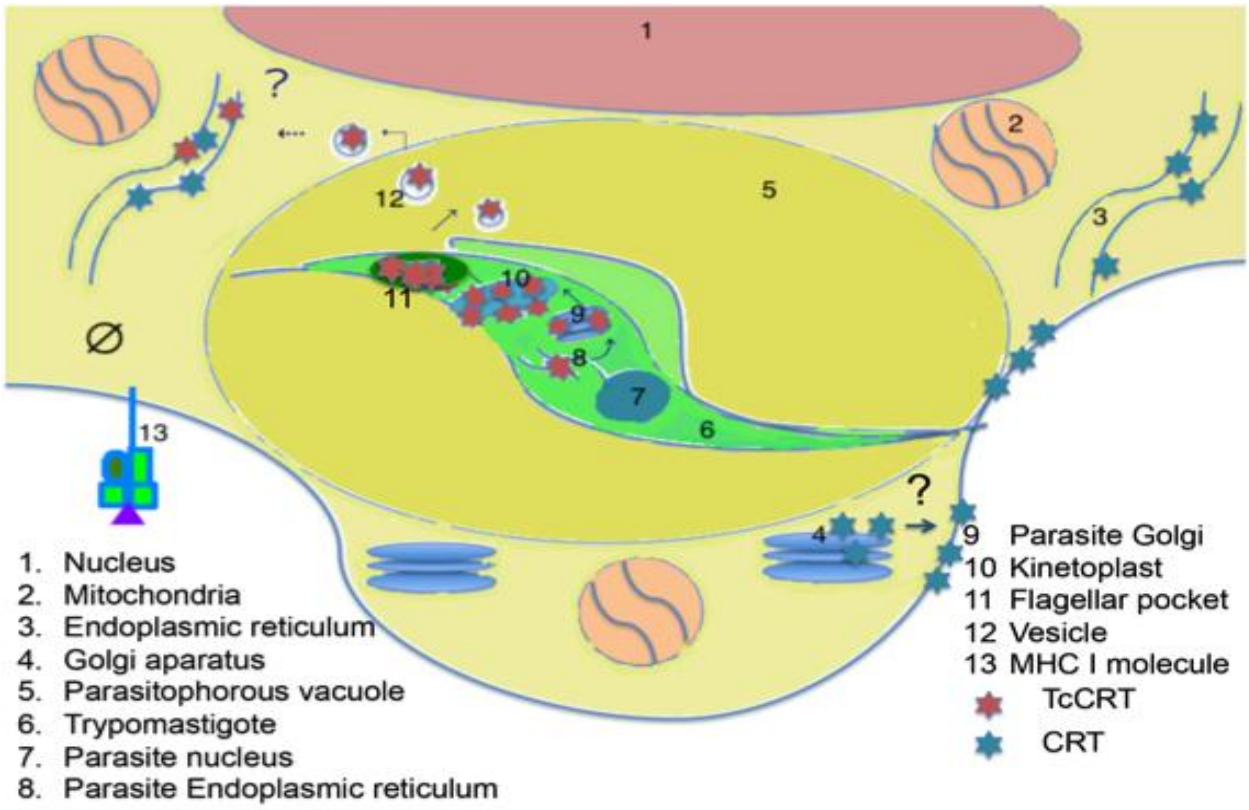

Figure 22: Proposed Model of Possible TcCRT Externalization *inside* Host Cells

Possible TcCRT route would includes several organelles like parasite's ER, Golgi and kinetoplast, as well as possible effects on the host cell CRT. From the parasite ER, TcCRT suffers post-translational modifications in the Golgi apparatus and then it accumulates in the kinetoplast, before it accesses to the flagellum pocket. Secretion to the parasite exterior follows possibly through micro vesicles. Once in the host cell cytoplasm, it could have functional implications such as down regulation of MHC-I molecules, or promoting MmCRT over expression.

If TcCRT binds to host cell MHC-I molecules with higher affinity than cellular CRT, it could down regulate the MHC-I expression on the host cell surface, a possibility consistent with our results. An immune evasive mechanism would thus be established. Several of these questions are addressable in current or future investigations in our laboratory.

SUMMARY OF PRINCIPAL RESULTS

- Two antibodies were suitable to be used as TcCRT detector probes in Immunocytochemistry. Monoclonal and polyclonal anti-TcCRT. The third antibody tested (anti-TcS) was not used because it showed significant cross-reactivity with a putative 46 kDa MmCRT.

- Topographic controls performed for each condition were properly resolved in electron microscopy.

- With the polyclonal anti-TcCRT, gold particles were observed in the non-infected host cell and free parasites.

- In infected cells, the label was observed in the host cell and parasitophorous vacuole, in parasite organelles that are consistent with previous results shown in free parasites.

- Vesicle-like structures with positive gold-label were observed in free trypomastigotes and infected cells.

- When infected, the density of gold particles is higher in different compartments of the host cell.

- With the monoclonal E2G7 anti-TcCRT, gold particles were detected in free parasites, in organelles consistent with previous results with the polyclonal antibody.

- On infected cells, in all conditions analyzed, the common pattern is a high-density label on the parasite kinetoplast, which is consistent with previous results obtained with the polyclonal anti-TcCRT antibody.

- The number of gold particles in kinetoplast sections is higher in parasites present in infected cells.

- The number of MHC-I positive cells decreases at 2 and 4, but not at 6h PI. As the percentage of fluorescence intensity remained similar between the samples, no variation in the number of MHC-I molecules per cell is observed.

CONCLUSIONS

- This is the first study where a parasitic chaperone molecule as TcCRT is detected *in situ* once the parasite is *inside* the host cell.

- The results presented here were validated by using two different antibodies, with common characteristics in its subcellular localization, in parasite organelles consistent with a secretory pathway.

- A correlation between the number of CRT molecules in cytoplasm and the number of MHC-I positive cells is detected post-infection, whereas the expression of MHC-I molecules per cell remained similar in all samples.

- This allows us to propose a model for TcCRT itinerary once the parasite is inside the host cell, in which two possible alternatives of functional implications of TcCRT inside the infected host-cell are presented.

- Hypothesis I was satisfied since TcCRT was detected in parasites *inside* the host cell.

- Hypothesis II was not satisfied, since an inverse correlation was detected between the number of CRT molecules and MHC-I positive cells, not with the number of MHC-I surface molecules.

ANNEX I: Detection of Possible *Mus musculus* Calreticulin (MmCRT) Isoforms in Different Murine Whole Cell Extracts (WCE)

MATERIALS AND METHODS

1.- Biological Material

1.1 Cell Lines

- RAW 264.7 murine macrophages (see Methods section 1.1).

- WT (K41) and *CRT* -/- (K42) cell lines, kindly donated by Dr. Marek Michalak, University of Alberta, Canada [43].

1.2 Recombinant Calreticulin (rTcCRT)

- rTcCRT (see Methods section 1.3).

1.3 Polyclonal Antibodies (PoAb)

- Anti-TcCRT/Anti-TcS (see Methods section 1.4).

2.- Reagents

- BioRad (USA): acrylamide, Bio-Rad Protein Assay, bis-acrylamide, ammonium persulphate, N,N,N',N'-tetramethylethylenediamine (TEMED).
- Calbiochem (USA): protease inhibitor cocktail.
- Dako (USA): Goat anti-rabbit IgG conjugated to horseradish peroxidase (HRP), goat anti-rabbit IgG conjugated to alkaline phosphatase (AP).
- GE-Healthcare (USA): Amersham hybond-ECL nitrocellulose membrane.
- Gibco (USA): L-glutamine, penicillin-streptomycin, trypsine.
- Hyclone (USA): Fetal bovine serum (FBS), RPMI medium, Dulbecco modified Eagle's medium (DMEM).
- Kodak (USA): BioMax Light Film 13x18 cms.
- MERCK (GER): Chlorhydric acid, Bromophenol blue, sodium bicarbonate,

sodium carbonate, sodium chloride, ethanol, sodium hydroxide, sodium azide, methanol.

- New England Biolabs (USA): Colour-plus pre-stained protein marker, broad range.
- Novus Biologicals (USA): Polyclonal antibody anti-CRT.
- Pierce (USA): Kit ECL Western Blot Substrate.
- Siemens (GER): Chassis Siemens 18x24 cms.
- Sigma-Aldrich: (USA): BSA, Coomassie blue R250, 2-mercaptoethanol, NBT-BCIP, paraformaldehyde, SDS, Tris-base, Tween 20.

3.- Methods

3.1 K41-K42 WCE Preparation

K41 and K42 *CRT* -/- murine fibroblast were cultured in Dulbecco Modified Eagle's Medium (DMEM) (Hyclone, USA), supplemented with 10% v/v FBS (Hyclone, USA), 1% v/v penicillin/streptomycin (Gibco, USA) and 1% v/v L-Glutamine (Gibco, USA). $1x10^7$ cells were harvested, washed 3 times and pellet was resuspended in 1 ml of PBS. 30 μl of TRITON X-100 and of protease inhibitor cocktail (Calbiochem, USA) were added to the cell preparation and mixture was placed on ice for 15 min Sonication of the mixture was performed for 20 sec at frequency Nº3 in Microson ultrasonic cell disruptor (Misonix, USA). A final centrifugation of the extract was performed at 16,170 *g* for 25 min to remove any cell debris and supernatant was stored at -20ºC. Protein concentration was measured by Bradford [62].

3.2 SDS-PAGE/IWB

3.2.1 SDS/PAGE

10 ng of rTcCRT and/or 30 μg of K41 or K42 WCE were separated through 12% polyacrylamide gel electrophoresis in Mini-Protean-2 chamber (BioRad, USA). Samples were heated at 100ºC in protein loading buffer 1x and then loaded in the gel. The electrophoresis ran at 100V and once finalized, the gel was transferred to a nitrocellulose membrane for IWB.

3.2.2 IWB

Previously separated proteins were transferred to nitrocellulose membranes, using a humid system, at 4ºC for 1h at 100V. Then, the membrane was blocked overnight at 4ºC in PBS with 5% w/v nonfat milk. The blocked membrane was incubated for 1.5h with anti-TcCRT, anti-TcS or anti-MmCRT PoAbs (see Methods section 1.4 and 2), diluted in PBS with nonfat milk 3% w/v. The membrane was washed 4 times with PBS in 0.05% v/v Tween 20 and then incubated with an anti-rabbit conjugated to AP, diluted 1/1,000 v/v or with anti-rabbit IgG conjugated to HRP in PBS 1 with 3% w/v nonfat milk for 1.5h at room temperature. The membrane was washed and enzymatic reaction mediated by the antibody union was detected with NBT-BCIP for AP conjugated antibodies, and in case of HRP conjugated antibody, positive reaction was identified through chemiluminescence using ECL Western Blot Substrate kit (Pierce, USA) with luminol and H_2O_2 and subsequent exposure to photographic plate (Pierce, USA).

3.3 Uni-Dimensional Electrophoresis for Mass Spectrometry

3.3.1 SDS-PAGE

Performed as described in the ANNEX I Section 3.2.1, with some modifications. 30 □g of RAW WCE (in quadruplicate) were separated through 12% polyacrylamide gel electrophoresis in Mini-Protean-2 chamber (BioRad, USA). Samples were heated at 100ºC in charge buffer and then loaded in the gel. The electrophoresis ran at 100V and once finalized, the gel was stained with Coomassie Blue. In parallel, other gel containing 30 μg of RAW 264.7 WCE was transferred to a nitrocellulose membrane for IWB procedures.

3.3.2 IWB

Performed as described in the ANNEX I Section 3.2.2. The primary antibody was the PoAb anti-TcS.

Coincident bands detected between the SDS-PAGE and IWB were cut and sent

to Mass spectrometry analysis.

3.4 Mass Spectrometry

3.4.1 MALDI-TOF

3.4.1.1 Sample Preparation

In brief, samples were washed three times with nanopure water for 30 min at room temperature, deinked with 200 mM ammonium bicarbonate prepared in 50% v/v acetonitrile for 30 min at 37°C. Then were incubated with DTT 10 mM prepared in 200 mM ammonium bicarbonate for 30 min at 37ºC and alkylated with 55 mM iodoacetamide prepared in 200 mM ammonium bicarbonate for 30 min at 37°C (in darkness). Samples were dehydrated with acetonitrile and dried at room temperature for 10 min and then placed on ice. Proteolysis buffer (50 mM ammonium bicarbonate/10% v/v acetonitrile containing 0.3 μg/μl of trypsin) was added (Promega Corp., USA) and mixture incubated on ice for 45 min Then proteolysis buffer was added (without trypsin) and incubated overnight at 37°C. The supernatant was recovered, two extractions were carried out with 60 % v/v acetonitrile, 0.1 % v/v formic acid and one extraction with acetonitrile. The supernatant and extractions were combined and taken to dryness in SpeedVac at room temperature. Concentrated samples were resuspended in 12 μl of 0.1 % v/v formic acid with 3% v/v methanol.

3.4.1.2 Spectra Acquisition

Each sample was mixed with matrix acid α -cyano-4-hydroxycinnamic acid (CHCA) in ratio 1:1 and 2 μL of each mixture was placed in a scout micro sample holder (Bruker Daltonics Inc., USA). Mass spectra were acquired in the MALDI-TOF equipment Microflex (Bruker Daltonics Inc., USA) in positive ion mode using reflection detection. Previous acquisition of the data a calibration of the equipment was performed with a external standard corresponding to a mixture of peptides 1000-3000 Da mass spectrometer (Bruker Daltonics Inc., USA). The final spectra correspond to the sum of 15 scans of 30 laser shots applied

at different points taken randomly from each sample deposited on the holder plate.

3.4.1.3 Spectrum Analysis

To analyze the spectra, flexAnalysis version 2.2 program was used (Bruker Daltonik GmbH, Germany). For detection of the monoisotopic m/z signal the SNAP algorithm (sophisticated numerical annotation procedure) was used. Once generated the monoisotopic m/z signals list, internal calibration was performed using the product signals of the auto proteolysis of trypsin, which were removed from the list and the remaining signals exported to Excel. Additionally, the list of exported masses of each sample was examined through the Peak Erazor 2.0.1 program (Lighthouse Data, Odense, DNK) in search of contamination with keratin, signals which were also removed from the list.

For identification of the acquired data, online Mascot program was employed(http://www.matrixscience.com/cgi/search_form.pl?FORMVER=2&SEARCH=PMF) using the following parameters: Proteolytic enzyme, trypsin; Loss cuts, 1; Stable modification, carbamidomethylation (alkylation with iodoacetamide); Variable modification, oxidation of methionine; Mass, monoisotopic; Mass tolerance, 0.1-0.3 Da. Analysis were performed without taxonomy restriction or restriction considering *Mus musculus*.

3.4.2 HPLC-Ion Trap

3.4.2.1 Spectra and Chromatograms Acquisition

After proteolysis of the samples, they were examined by LC-MS system consisted of Agilent HPLC chromatograph 1100 (Agilent Technologies Inc., USA) coupled to an electrospray-ion trap mass spectrometer ESI-TRAP ionic Esquire 4000 (Bruker Daltonik GmbH, GER). To control the HPLC chromatograph, the LC 3D Rev.A.10.02 ChemStation program was used (Agilent Technologies Inc., USA) and for controlling the mass spectrometer the esquireControl 5.2 software was used (Bruker Daltonik GmbH, GER).

For HPLC separation a C18 column of 150 × 0.3 mm, 4 um and 90 Å was used (Jupiter - Proteus, Phenomenex Inc., USA), the outlet of which was connected directly to the mass spectrometer. The separation of 20 μl of each sample was performed at room temperature. The electrospray-mediated ionization process (fogging) was performed at 4000V with nitrogen as nebulizer gas at 300°C, 20 psi pressure and flow rate of 5 L/min Mass spectra were acquired in positive polarity.

3.4.2.2 Chromatogram Analysis and Proteins Identification

For chromatograms and spectra analysis, DataAnalysis program version 3.2 was used (Bruker Daltonik GmbH, GER). Data was generated using the Compounds–AutoMSn options, which allowed the detection of m/z signals and corresponding fragmentations.

For identification of the acquired data, Online Mascot Program was used (http://www.matrixscience.com/search_form_select.html) through the MS/MS Ion Search option. The following restrictions were considered for identification: Proteolytic enzyme, trypsine; Loss of cuts, 1; Stable modification, carbamidomethylation (alkylation with iodoacetamide); Variable modification, oxidation of methionine; Mass, monoisotopic; Mass tolerance, 0.8 Da; Tolerance fragmentation, 0.8 Da; Peptide charge, 1 +, 2 + and 3 + , and Instrument, ESI - TRAP. The analysis was performed using unrestricted taxonomy or *Mus musculus*. Same studies were performed with the MmCRT sequence.

3.4.3 Sequence Analysis

Sequences corresponding to m/z signals that were concordant to MmCRT, were analyzed with Online ClustalW program (http://www.ebi.ac.uk/Tools/msa/clustalw2/).

4.- Services

Sample processing, Mass spectra acquisition and Spectra analysis were performed in Mass Spectrometry Unit, Faculty of Chemical and Pharmaceutical Sciences, University of Chile.

RESULTS

1. SDS-PAGE/IWB

- **Detection with anti-TcS PoAbs in murine macrophages**

The third antibody to be tested as a potential detector probe is the anti-TcS PoAb. When a RAW 264.7 WCE was incubated with this antibody, a 46 kDa molecule was observed in all dilutions employed (Fig. 23).

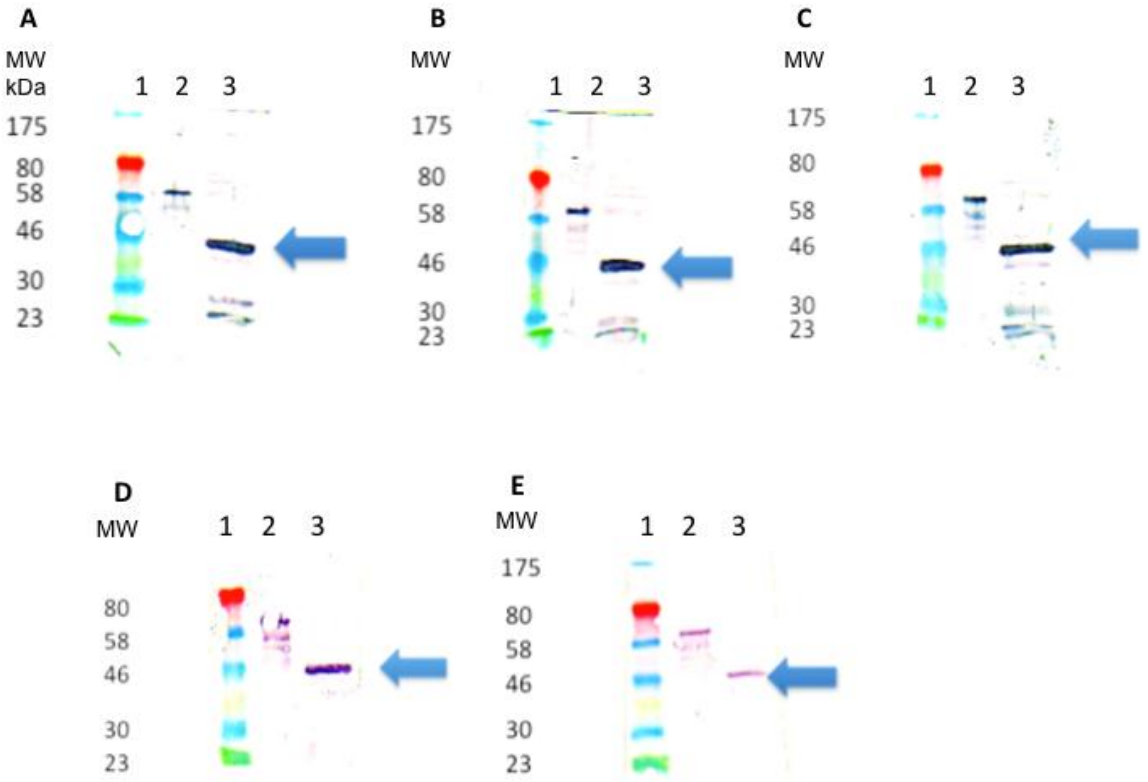

Figure 23: A Polyclonal Anti-TcS Serum Detects a 46 kDa Molecule, Antigenically Homologous with MmCRT

In a murine macrophage WCE, a 46 kDa putative MmCRT is detected at different anti-TcS dilutions (v/v) **A:** 1/1,000, **B:** 1/2,000, **C:** 1/4,000**, D:** 1/8,000, and **E:** 1/16,000.

A-E: Lane 1: Molecular weight standard, lane 2**:** rTcCRT, lane 3**:** RAW 264.7 WCE. Arrows: 46 kDa putative MmCRT.

The former result raised interesting questions regarding the existence of a second MmCRT isoform. This is sustained by the fact that a second *MmCRT* gene was described [63]. Also, in a collaboration with Dr. Patricia Cogram, this molecule was also observed in IWB of murine brain WCE (data not shown).

In order to validate the former results, a murine fibroblast deficient in MmCRT (K42 cell line) was evaluated with the available antibodies, as compared to the WT murine fibroblast (K41 cell line).

- **Detection with anti-TcCRT PoAbs in murine fibroblasts**

Several proteins are detected in K41 and K42 cell lines (Fig.24) when this polyclonal antibody is employed, one of which consistent with previously analyzed RAW 264.7 WCE (58 kDa).

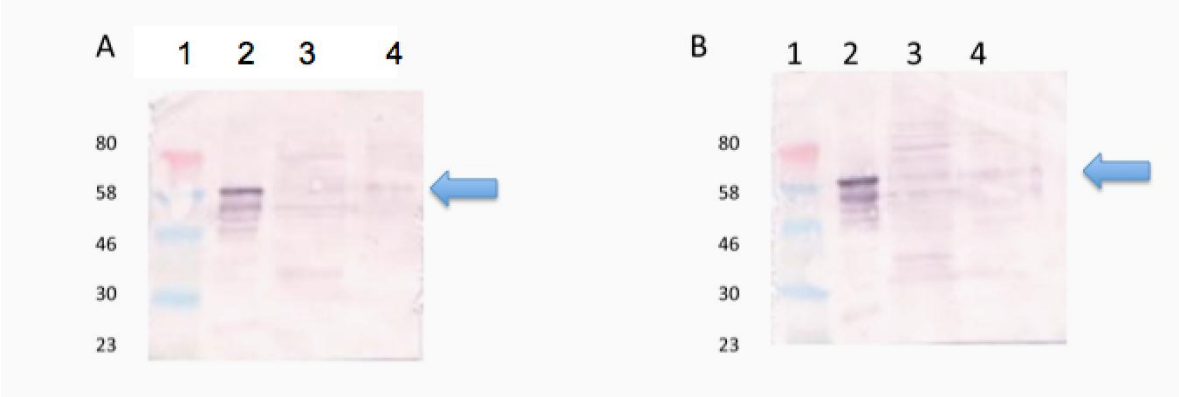

Figure 24: Anti-TcCRT PoAbs Recognize Several Proteins in K41 and K42 WCE.

In murine fibroblasts WCE, several proteins are detected by cross reactivity with an anti-TcCRT PoAb at dilution (v/v): **A:** 1/2,000, **B:** 1/8,000, among which the 58 kDa molecule is observed.

A-B: Lane 1: Molecular weight standard, lane 2: rTcCRT, lane 3: K41 WCE, lane 4: *CRT -/-* K42 WCE. Arrow: 58 kDa putative MmCRT.

- **Detection with anti-TcS PoAbs in murine fibroblasts**

When the anti-TcS PoAb was employed, several proteins were recognized in K41 and K42 WCE (Fig. 25), among which the 46 kDa molecule highlights. These results are consistent with previous results obtained with the RAW 264.7 WCE.

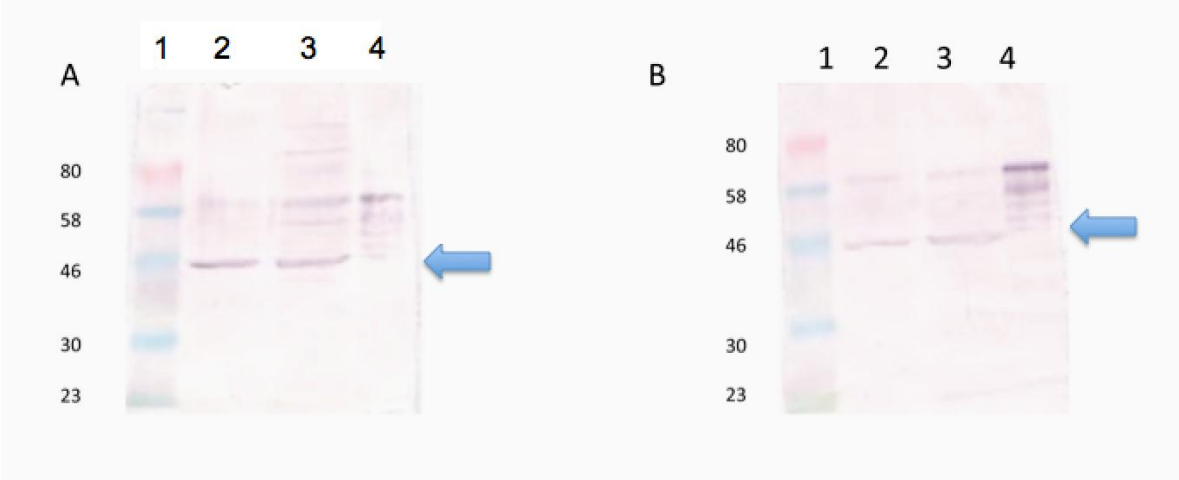

Figure 25: Anti-TcS PoAbs Recognize Several Proteins in K41 and K42 WCE, among which the 46 kDa Band highlights.

In murine fibroblast WCE incubated with the anti-TcS PoAb (v/v): **A:** 1/2,000, **B:** 1/8,000, several proteins are detected by cross reactivity, among which the 46 kDa putative MmCRT highlights.

A-B: Lane 1: Molecular weight standard, lane 2: *CRT* -/- K42 WCE, lane 3: K41 WCE, lane 4: rTcCRT. Arrow: Putative 46 kDa MmCRT.

- **Detection with homologous anti-MmCRT PoAb in murine WCE**

With the homologous anti-MmCRT PoAb, the 58 kDa MmCRT was detected only in *CRT* +/+ extracts (RAW 264.7 and K41 WCE). No band was detected in the K42 WCE (Fig. 26), consistent with previous results [43].

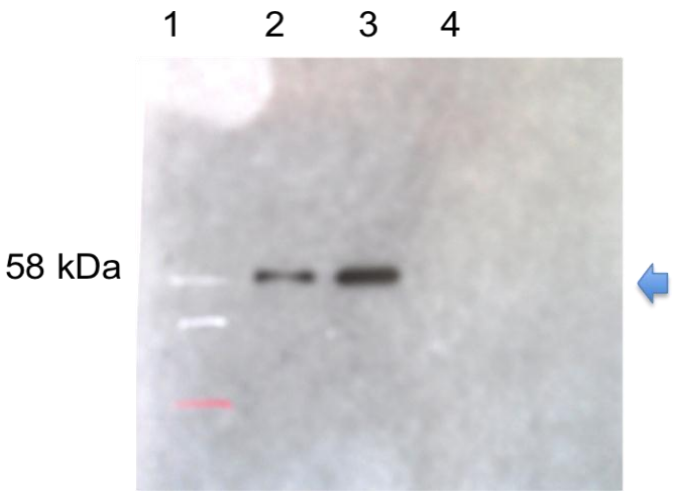

Figure 26: Anti-MmCRT PoAb Recognize MmCRT only in *CRT* +/+ WCE (RAW 264.7 and K41)

When the three murine WCE generated are incubated with the homologous commercial anti-MmCRT PoAb (1/500 v/v) only in the *CRT* +/+ WCE the molecule is detected

Lane 1: Molecular weight standard, lane 2: RAW 264.7 WCE, lane 3: K41 WCE, lane 4: *CRT* -/- K42 WCE.

Taken together, these results suggest that there is cross-recognition of a 46 kDa band with the anti-TcS polyclonal serum, consistent with the possibility of a CRT-like molecule in three murine WCE.

2.- Uni-dimensional Electrophoresis/Mass Spectrometry

- **46 kDa Band Analysis**

From an uni-dimensional SDS/PAGE electrophoresis, the 46 kDa band was cut from a coomassie-blue stained gel, using as reference an IWB performed in parallel (Fig. 27).

The sample was processed for MALDI-TOF mass spectrometry analysis, in which one peptide was concordant with MmCRT, with 100% of identity (Figs. 28-29). However, since a 7 amino acid peptide is not sufficient to identify the protein, the sample was also processed for an HPLC-ION TRAP mass spectrometry analysis. In this case, 2 peptides were obtained, each with a 100% identity when compared to MmCRT.

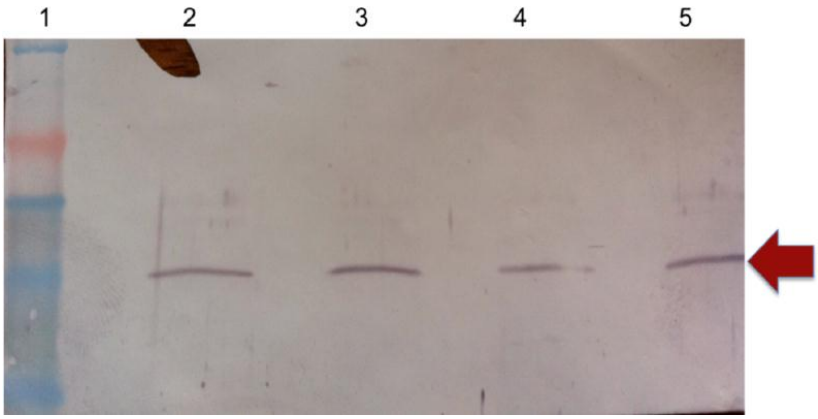

Figure 27: Anti-TcS PoAbs Recognize a 46 kDa Immunoreactive Band in RAW 264.7 WCE.

Reference IWB of SDS-PAGE gel stained and cut for mass spectrometry.

Anti-TcS 1/2,000 v/v; lane 1: Molecular weight standard, lanes 2-5: RAW 264.7 WCE. Immunoreactive band of 46 kDa is observed (arrow).

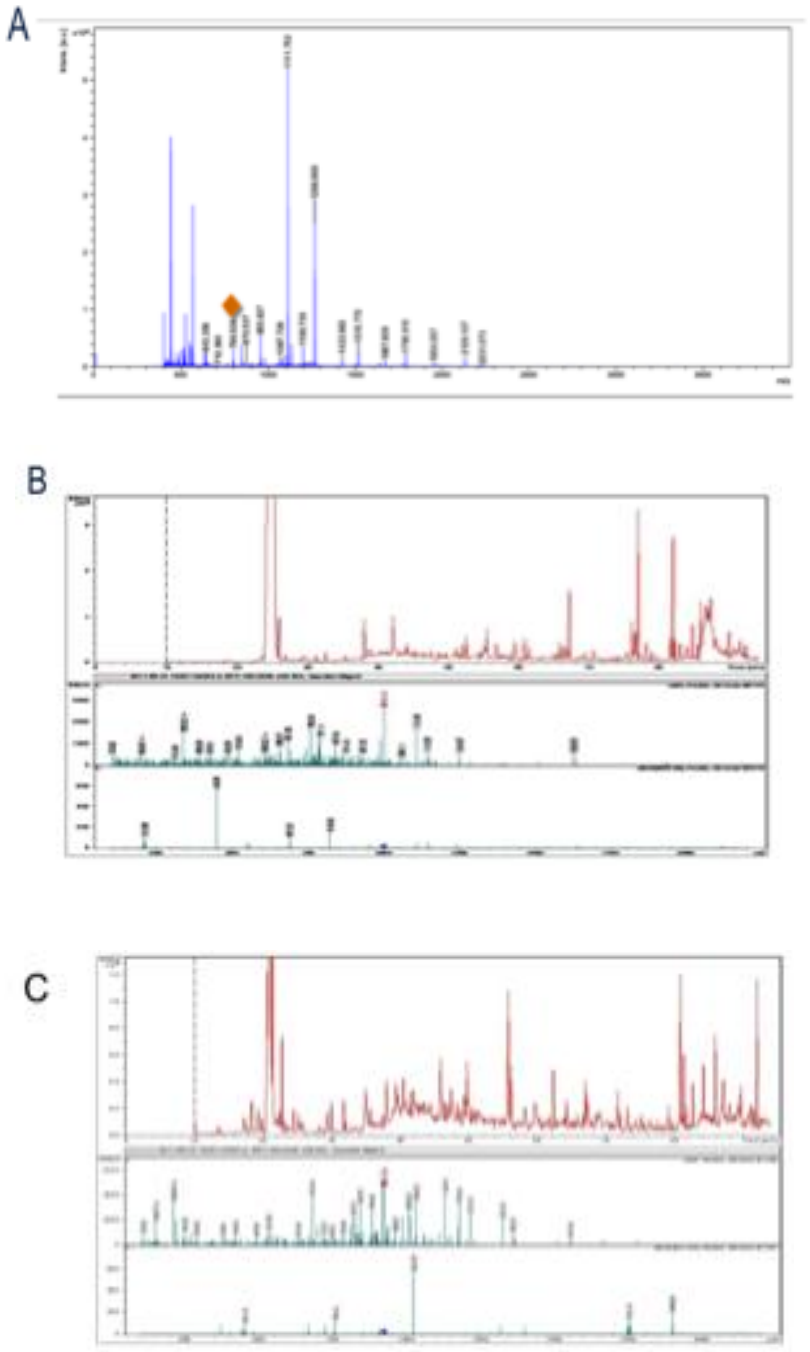
A
B
C

Figure 28: Three peptides, Concordant with MmCRT, are Detected in the 46 kDa Band, from RAW 264.7 WCE.

A: Mass Spectrum of peptides obtained by MALDI-TOF from the protein of 46 kDa (intensity vs. mass/charge (m/z)). Rhomb: first signal corresponding to peptide consistent with MmCRT. **B-C:** Mass Spectra obtained by HPLC-ion-trap. In each figure are presented in the following order: HPLC chromatogram (intensity vs. time) spectrum obtained without peptide fragmentation (intensity versus mass/charge (m/z)), and fragmented peptides spectrum (intensity versus m/z). Rhombuses indicate signals corresponding to peptides 2 and 3 concordant with MmCRT.

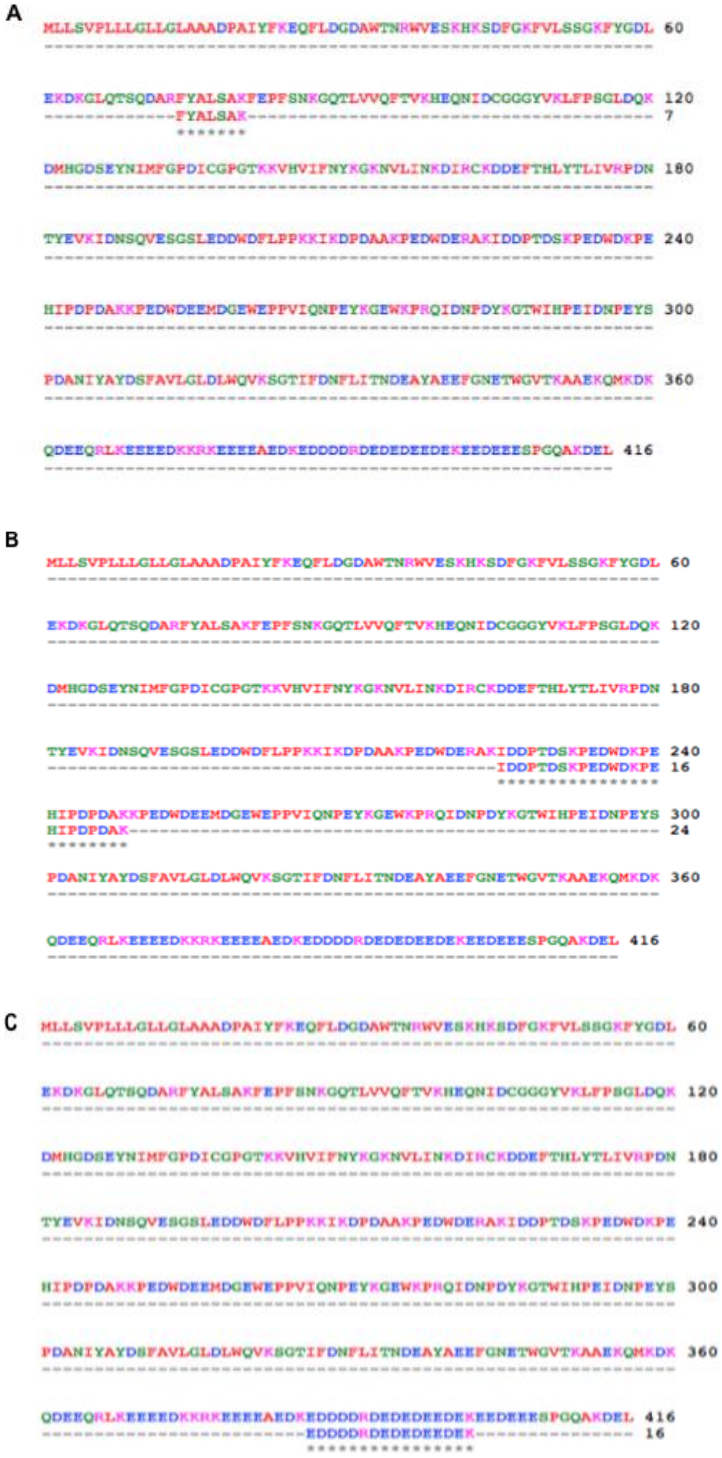

Figure 29: Peptides Obtained by Mass Spectrometry from the RAW 264.7 WCE 46 kDa band, are Identical with the Amino Acid Sequence Described for MmCRT.

A: Peptide 1, obtained by MALDI-TOF, N domain (aa 74-80), **B:** Peptide 2 obtained by HPLC-ion trap, P domain (aa 225-248), **C:** Peptide 3, obtained by HPLC-ion trap, carboxy-terminus (aa 386-401) All alignments were performed using the CLUSTAL-W program, each peptide with 100% identity with MmCRT.

DISCUSSION

In three different murine WCE (including a CRT -/- murine fibroblast), a 46 kDa molecule, possibly a MmCRT isoform, is detected by the anti-TcS PoAb (Fig 24-25 and 27). When the homologous anti-MmCRT is employed, the 58 kDa MmCRT was detected only in the extracts generated with CRT +/+ cell lines (Fig.26).

In the 46 kDa band, 3 peptides 100% identical to MmCRT aminoacidic sequence were detected. Since these three peptides contain 47 amino acids representing only 11% of the MmCRT sequence, they constitute only a modest indication of the presence of MmCRT in the analysed sample (Fig.28-29).

In this regard, it must be considered that the samples employed for this analysis were direct murine WCE, not a molecule purified by any method, which made difficult a full identification.

In a series of additional experiments, not shown in this document, but available for the Thesis Committee examination, a Bi-dimensional electrophoresis/Mass spectrometry analysis of murine WCE (RAW 264.7, K42) was used. Nine additional peptides, different from those previously found, were detected, spanning a total of 96 amino acids, equivalent to 24 % of the molecule in the K42 sample, and 105 amino acids, equivalent to a 26% of the molecule in the RAW 264.7 sample. Again, these results are a suggestion that a second MmCRT molecule exists in RAW 264.7 and K42 cells. Unfortunately, the FDR index (a measure of the reliability of the positive signals obtained) was too high in these experiments.

If a second MmCRT form does exist, several important implications could be proposed: **i).** The putative 46 kDa molecule should be the product of a second gene, rather than the spliced form of a single structural gene, which is consistent with the reports that showed a second MmCRT gene [63]. **ii).** In the CRT deficient murine fibroblast cell line (K42), the presence of the putative isoform is compatible with the reported inactivation of the gene coding for the 58 kDa CRT molecule. **iii).** Related with ii), and given the functional polymorphism of CRT in cell vitality, the presence of the 46 kDa isoform in the deficient cell line, could explain its survival *in vitro,* in spite

of the extensive morphological alterations detected in TEM.

CONCLUSIONS

- The 46 kDa molecule, antigenically homologous with MmCRT, was detected in at least 3 different murine WCE, including a *CRT* -/- deficient murine fibroblast with the Anti-TcS PoAb.

- In the 46 kDa molecule, three peptides 100% identical with MmCRT aminoacidic sequence, were detected by Mass Spectrometry.

- Additional experiments performed (but not shown in this section) through bi-dimensional electrophoresis to achieve full identification of the molecule were positive, obtaining a 24% of MmCRT amino acid sequence. However the FDR index (an indicator that evaluates the trustworthiness of the positive signals obtained) was high, so the reliability of these results is low.

- There is a modest indication of the presence of a second MmCRT molecule that weights 46 kDa. No full identification was possible with the available techniques.

REFERENCES

1. Clayton, J., *Chagas disease 101.* Nature, 2010. **465**(7301): p. S4-5.

2. Clayton, J., *Chagas disease: pushing through the pipeline.* Nature, 2010. **465**(7301): p. S12-5.

3. Coura, J.R. and P.A. Vinas, *Chagas disease: a new worldwide challenge.* Nature, 2010. **465**(7301): p. S6-S7.

4. Sarkar, S., et al., *Chagas disease risk in Texas.* PLoS Negl Trop Dis, 2010. **4**(10).

5. Bern, C. and S.P. Montgomery, *An estimate of the burden of Chagas disease in the United States.* Clin Infect Dis, 2009. **49**(5): p. e52-4.

6. Hotez, P.J., et al., *Chagas disease: "the new HIV/AIDS of the Americas".* PLoS Negl Trop Dis, 2012. **6**(5): p. e1498.

7. Schmunis, G.A., *Epidemiology of Chagas disease in non-endemic countries: the role of international migration*, in *Mem. Ins. Oswaldo Cruz*. 2007. p. 75-85.

8. Yoshida, N., *Trypanosoma cruzi infection by oral route: how the interplay between parasite and host components modulates infectivity.* Parasitol Int, 2008. **57**(2): p. 105-9.

9. Toso, M., Vial, F., Galanti, N., , *Transmisión de la enfermedad Chagas por vía oral.* Revista Médica de Chile, 2011. **139**: p. 258-66.

10. Michalak, M., et al., *Calreticulin: one protein, one gene, many functions.* Biochem J, 1999. **344 Pt 2**: p. 281-92.

11. Paulsson, K. and P. Wang, *Chaperones and folding of MHC class I molecules in the endoplasmic reticulum.* Biochim Biophys Acta, 2003. **1641**(1): p. 1-12.

12. Mancino, L., et al., *Calreticulin recognizes misfolded HLA-A2 heavy chains.* Proc Natl Acad Sci U S A, 2002. **99**(9): p. 5931-6.

13. Eggleton, P. and M. Michalak, *Calreticulin for better or for worse, in sickness and in health, until death do us part.* Cell Calcium, 2013. **54**(2): p. 126-31.

14. Ferreira, V., et al., *Role of calreticulin from parasites in its interaction with vertebrate hosts.* Mol Immunol, 2004. **40**(17): p. 1279-91.

15. Ferreira, V., et al., *The classical activation pathway of the human complement system is specifically inhibited by calreticulin from Trypanosoma cruzi.* J Immunol, 2004. **172**(5): p. 3042-50.

16. Ramirez, G., et al., *Extracellular Trypanosoma cruzi calreticulin in the host-parasite interplay.* Trends Parasitol, 2012. **27**(3): p. 115-22.

17. Ramirez, G., et al., *Trypanosoma cruzi calreticulin: a novel virulence factor that binds complement C1 on the parasite surface and promotes infectivity.* Immunobiology, 2011. **216**(1-2): p. 265-73.

18. Lopez, N.C., et al., *Antiangiogenic and antitumor effects of Trypanosoma cruzi Calreticulin.* PLoS Negl Trop Dis, 2010. **4**(7): p. e730.

19. Molina, M.C., et al., *An in vivo role for Trypanosoma cruzi calreticulin in antiangiogenesis.* Mol Biochem Parasitol, 2005. **140**(2): p. 133-40.

20. Ferreira, V., et al., *Does Trypanosoma cruzi calreticulin modulate the complement system and angiogenesis?* Trends Parasitol, 2005. **21**(4): p. 169-74.

21. Jannin, J. and L. Villa, *An overview of Chagas disease treatment.* Mem Inst Oswaldo Cruz, 2007. **102 Suppl 1**: p. 95-7.

22. Prata, A., *Clinical and epidemiological aspects of Chagas disease.* Lancet Infect Dis, 2001. **1**(2): p. 92-100.

23. Mario Faúndez, R.L.-M., Gloria Torres,Antonio Morello,Jorge Ferreira, Ulrike Kemmerling, Myriam Orellana and Juan D. Maya*, *Buthionine Sulfoximine Has Anti-Trypanosoma cruzi Activity in a Murine Model of Acute Chagas' Disease and Enhances the Efficacy of Nifurtimox.* Antimicrob Agents Chemother, 2008. **52**(5): p. 1837-9.

24. Juan Diego Maya , M.O., Jorge Ferreira, Ulrike Kemmerling, Rodrigo López-Muñoz and Antonio Morello, *Chagas disease: Present status of pathogenic mechanisms and chemotherapy.* Biological Research, 2010. **43**(3): p. 323-331.

25. Viotti, R., et al., *Side effects of benznidazole as treatment in chronic Chagas disease: fears and realities.* Expert Rev Anti Infect Ther, 2009. **7**(2): p. 157-63.

26. Castro, J.A., M.M. de Mecca, and L.C. Bartel, *Toxic side effects of drugs used to treat Chagas' disease (American trypanosomiasis).* Hum Exp Toxicol, 2006. **25**(8): p. 471-9.

27. Poli, P., et al., *Cytotoxic and genotoxic effects of megazol, an anti-Chagas' disease drug, assessed by different short-term tests.* Biochem Pharmacol, 2002. **64**(11): p. 1617-27.

28. Eggleton, P., Michalak, M., *Calreticulin*. Second Edition ed. 2003: Landes Bioscience/ Plenun Publishers.

29. Chagas, C., *Nova tripanozomiase Humana. Estudos sobre a morfología e o ciclo evolutivo do Schizotrypanum cruzi, n. gen., n. sp., ajente etiológico de nova entidade morbida do homen.* Mem. Inst. Oswaldo Cruz, 1909. **1**(2): p. 159-218.

30. Ley, V., et al., *Amastigotes of Trypanosoma cruzi sustain an infective cycle in mammalian cells.* J Exp Med, 1988. **168**(2): p. 649-59.

31. http://www.dpd.cdc.gov/dpdx/HTML/ImageLibrary/TrypanosomiasisAmerican_il.htm.

32. Johnson, S., Michalak, M., Opas, M., Eggleton, P., *The Ins and Outs of Calreticulin: from the ER lumen to the Extracellular Space.* Trends Cell Biol, 2005. **11**(3): p. 122-129.

33. Corbett, E.F., et al., *Ca2+ regulation of interactions between endoplasmic reticulum chaperones.* J Biol Chem, 1999. **274**(10): p. 6203-11.

34. Sonnichsen, B., et al., *Retention and retrieval: both mechanisms cooperate to maintain calreticulin in the endoplasmic reticulum.* J Cell Sci, 1994. **107 (Pt 10)**: p. 2705-17.

35. Antoniou, A.N. and S.J. Powis, *Pathogen evasion strategies for the major histocompatibility complex class I assembly pathway.* Immunology, 2008. **124**(1): p. 1-12.

36. Roder, G., et al., *Viral proteins interfering with antigen presentation target the major histocompatibility complex class I peptide-loading complex.* J Virol, 2008. **82**(17): p. 8246-52.

37. Spooner, R.A., et al., *Retrograde transport pathways utilised by viruses and protein toxins.* Virol J, 2006. **3**: p. 26.

38. Smith, D.C., et al., *Internalized Pseudomonas exotoxin A can exploit multiple pathways to reach the endoplasmic reticulum.* Traffic, 2006. **7**(4): p. 379-93.

39. Afshar, N., B.E. Black, and B.M. Paschal, *Retrotranslocation of the chaperone calreticulin from the endoplasmic reticulum lumen to the*

cytosol. Mol Cell Biol, 2005. **25**(20): p. 8844-53.

40. Burns, K., et al., *Modulation of gene expression by calreticulin binding to the glucocorticoid receptor.* Nature, 1994. **367**(6462): p. 476-80.

41. Dedhar, S., *Novel functions for calreticulin: interaction with integrins and modulation of gene expression?* Trends Biochem Sci, 1994. **19**(7): p. 269-71.

42. Dedhar, S., et al., *Inhibition of nuclear hormone receptor activity by calreticulin.* Nature, 1994. **367**(6462): p. 480-3.

43. Mesaeli, N., et al., *Calreticulin is essential for cardiac development.* J Cell Biol, 1999. **144**(5): p. 857-68.

44. Greives, M.R., et al., *Exogenous calreticulin improves diabetic wound healing.* Wound Repair Regen, 2012. **20**(5): p. 715-30.

45. Abbas, A.K., Litchman A.H, *Cellular and Molecular Immunology*. 5 ed, ed. C. Saunders. 2003.

46. Ferreira, A., Afani, A., Lanza, P., Aguillón, J.C, Sepúlveda, C., *Inmunología Básica y Clínica*. Mediterraneo, ed. 2005.

47. Aguillon, J.C., et al., *Tc45, a dimorphic Trypanosoma cruzi immunogen with variable chromosomal localization, is calreticulin.* Am J Trop Med Hyg, 2000. **63**(5-6): p. 306-12.

48. Ferreira, V., Molina, M.C, Valck, C., Ramirez, G., *Parasite Calreticulin: Possible Roles in the Parasite/Host Interface* Inmunología, 2002. **21**: p. 156-168.

49. Valck, C., et al., *Molecular mechanisms involved in the inactivation of the first component of human complement by Trypanosoma cruzi calreticulin.* Mol Immunol, 2010. **47**(7-8): p. 1516-21.

50. Ribeiro, C.H., et al., *Trypanosoma cruzi calreticulin: a possible role in Chagas' disease autoimmunity.* Mol Immunol, 2009. **46**(6): p. 1092-9.

51. Sanchez Valdez, F.J., et al., *Trypanosoma cruzi carrying a monoallelic deletion of the calreticulin (TcCRT) gene are susceptible to complement mediated killing and defective in their metacyclogenesis.* Mol Immunol, 2013. **53**(3): p. 198-205.

52. Sanchez-Valdez, F.J., et al., *A Monoallelic Deletion of the TcCRT Gene Increases the Attenuation of a Cultured Trypanosoma cruzi Strain,*

Protecting against an In Vivo Virulent Challenge. PLoS Negl Trop Dis, 2014. **8**(2): p. e2696.

53. Souto-Padron, T., C.A. Labriola, and W. de Souza, *Immunocytochemical localisation of calreticulin in Trypanosoma cruzi.* Histochem Cell Biol, 2004. **122**(6): p. 563-9.

54. Bayer-Santos, E., et al., *Proteomic analysis of Trypanosoma cruzi secretome: characterization of two populations of extracellular vesicles and soluble proteins.* J Proteome Res, 2012. **12**(2): p. 883-97.

55. Landfear, S.M. and M. Ignatushchenko, *The flagellum and flagellar pocket of trypanosomatids.* Mol Biochem Parasitol, 2001. **115**(1): p. 1-17.

56. Rodighiero, C., et al., *Role of ubiquitination in retro-translocation of cholera toxin and escape of cytosolic degradation.* EMBO Rep, 2002. **3**(12): p. 1222-7.

57. La Flamme, A.C., et al., *Trypanosoma cruzi-infected macrophages are defective in major histocompatibility complex class II antigen presentation.* Eur J Immunol, 1997. **27**(12): p. 3085-94.

58. Andrade, L.O. and N.W. Andrews, *Lysosomal fusion is essential for the retention of Trypanosoma cruzi inside host cells.* J Exp Med, 2004. **200**(9): p. 1135-43.

59. Aguilar, L., et al., *F(ab')2 antibody fragments against Trypanosoma cruzi calreticulin inhibit its interaction with the first component of human complement.* Biol Res, 2005. **38**(2-3): p. 187-95.

60. Aguillon, J.C., et al., *Recognition of an immunogenetically selected Trypanosoma cruzi antigen by seropositive chagasic human sera.* Acta Trop, 1997. **63**(2-3): p. 159-66.

61. Kohler, G. and C. Milstein, *Continuous cultures of fused cells secreting antibody of predefined specificity.* Nature, 1975. **256**(5517): p. 495-7.

62. Bradford, M., *A rapid and sensitive method for the quantitation of microgram quantities of protein utilizing the principle of protein-dye binding.* Anal. Biochem., 1976. **72**(1-2): p. 248-54.

63. Persson, S., M. Rosenquist, and M. Sommarin, *Identification of a novel calreticulin isoform (Crt2) in human and mouse.* Gene, 2002. **297**(1-2): p. 151-8.

64. Van Overtvelt, L., et al., *Trypanosoma cruzi down-regulates*

lipopolysaccharide-induced MHC class I on human dendritic cells and impairs antigen presentation to specific CD8(+) T lymphocytes. Int Immunol, 2002. **14**(10): p. 1135-44.

65. Buckner, F.S., B.T. Wipke, and W.C. Van Voorhis, *Trypanosoma cruzi infection does not impair major histocompatibility complex class I presentation of antigen to cytotoxic T lymphocytes.* Eur J Immunol, 1997. **27**(10): p. 2541-8.

66. Girard-Dias, W., et al., *On the ultrastructural organization of Trypanosoma cruzi using cryopreparation methods and electron tomography.* Histochem Cell Biol, 2012. **138**(6): p. 821-31.

67. Burns, K., et al., *Calreticulin: from Ca2+ binding to control of gene expression.* Trends Cell Biol, 1994. **4**(5): p. 152-4.

68. Shapiro, T.A. and P.T. Englund, *The structure and replication of kinetoplast DNA.* Annu Rev Microbiol, 1995. **49**: p. 117-43.

69. Simpson, L., *The mitochondrial genome of kinetoplastid protozoa: genomic organization, transcription, replication, and evolution.* Annu Rev Microbiol, 1987. **41**: p. 363-82.

70. Arnaudeau, S., et al., *Calreticulin differentially modulates calcium uptake and release in the endoplasmic reticulum and mitochondria.* J Biol Chem, 2002. **277**(48): p. 46696-705.

71. Tarr, J.M., et al., *A mechanism of release of calreticulin from cells* during *apoptosis.* J Mol Biol, 2010. **401**(5): p. 799-812.

72. Kuraishi, T., et al., *Identification of calreticulin as a marker for phagocytosis of apoptotic cells in Drosophila.* Exp Cell Res, 2007. **313**(3): p. 500-10.

73. Gardai, S.J., et al., *Cell-surface calreticulin initiates clearance of viable or apoptotic cells through trans-activation of LRP on the phagocyte.* Cell, 2005. **123**(2): p. 321-34.